nature sustainability

Article

https://doi.org/10.1038/s41893-025-01595-9

Conservation outcomes of dietary transitions across different values of nature

Received: 31 January 2024

Accepted: 11 June 2025

Published online: 3 October 2025

Check for updates

Patrick von Jeetze[1,2], Isabelle Weindl[1], Justin Andrew Johnson[3], Pasquale Borrelli[4,5], Panos Panagos[6], Tobias Meyer[7], Florian Humpenöder[1], Pascal Sauer[1], Jan Philipp Dietrich[1], Hermann Lotze-Campen[1,2] & Alexander Popp[1,8]

Conservation benefits from dietary change are commonly assessed without accounting for different conservation objectives. By representing fine-scale habitat and landscape change within a dynamic land-system model, we assess how a partial or full transition to healthier diets would affect indicators across the 'Nature for Nature' and 'Nature for Society' conservation value perspectives. We find that most diet-related conservation benefits are already achieved by a partial shift to healthier diets. This is because, particularly in many countries in tropical Africa and Asia, adopting healthier diets would mainly involve substituting staple foods with more varied plant-based foods rather than replacing resource-intensive livestock products. Conservation action in line with the Global Biodiversity Framework, by contrast, most consistently improves outcomes across both value perspectives, even under current demand trends, showing that spatial planning is central for decoupling conservation outcomes from food demand. However, any progress towards healthier diets not only lowers greenhouse gas emissions but also reduces barriers to effective conservation, such as higher food prices and imports.

Over the past century, unprecedented changes in both the character and scale of the land used for food production have made agriculture by far the most prominent driver of biodiversity loss[1,2]. Today, the food sector is also the primary driver of nitrogen pollution, freshwater consumption and soil degradation[3,4], while about one-third of all greenhouse gas (GHG) emissions are linked to the food system[5]. Population growth and the ongoing 'nutrition transition' with rising average incomes towards higher intakes of resource-intensive foods, particularly from livestock, could further escalate the environmental pressures of food production[6].

Recent assessments have shown that a reduction in the intake of resource-intensive livestock-based foods in favour of a variety of plant-based foods would not only provide substantial health benefits and a reduction in food-related mortality but also largely lower the massive environmental burden of food production[7,8]. In terms of biodiversity conservation, several studies have also suggested substantial benefits of a shift towards healthier diets, in particular owing to the enormous 'land-saving effect' as a result of changing agricultural demand[9,10]. However, conservation benefits from dietary change depend not only on the quantity of land that is protected from conversion but more importantly on the quality and location of conserved habitats[11–13]. Moreover, dietary changes may address specific conservation aspects, such as reducing the conversion of pristine habitats for feed production[14]. Yet, other aspects, such as the simplification

[1]Potsdam Institute for Climate Impact Research (PIK), Member of the Leibniz Association, Potsdam, Germany. [2]Albrecht Daniel Thaer-Institute of Agricultural and Horticultural Sciences, Humboldt University of Berlin, Berlin, Germany. [3]Department of Applied Economics, University of Minnesota, Saint Paul, MN, USA. [4]Environmental Geosciences, Department of Environmental Sciences, University of Basel, Basel, Switzerland. [5]Department of Science, Roma Tre University, Rome, Italy. [6]European Commission, Joint Research Centre (JRC), Ispra, Italy. [7]Department of Physical Geography and Ecosystem Science, Lund University, Lund, Sweden. [8]Faculty of Organic Agricultural Sciences, University of Kassel, Witzenhausen, Germany. e-mail: vjeetze@pik-potsdam.de

of landscapes with a long history of land use[15] and associated losses in nature's contributions to people (NCP)[2], are more closely connected to broader structural trends in food production, such as specialization, intensification and the concentration of agricultural land[16,17]. Hence, conservation benefits from dietary change may not only vary across space but may also differ across conservation perspectives, depending on whether the focus is on the intrinsic values of nature, such as preserving intact habitats, or its instrumental values, such as the supply of important NCP in managed landscapes. Consequently, some of the principles that apply to other environmental outcomes of food production, such as an approximately linear scaling of CH_4 and N_2O emissions with livestock production levels[18], may not necessarily extend to conservation outcomes in relation to shifts in food demand.

The aim of this study was to disentangle the impacts of dietary change across different conservation value perspectives, as illustrated in the Intergovernmental Science-Policy Platform on Biodiversity and Ecosystem Services (IPBES) Nature Futures Framework[19], in particular the 'Nature for Nature' (intrinsic) and 'Nature for Society' (instrumental) perspectives. We therefore applied a quantitative and spatially explicit modelling framework to assess how a shift towards healthier diets could affect indicators across these conservation perspectives at a spatial scale and detail of habitat representation that goes well beyond previous efforts[20,21] (Extended Data Table 1 and Extended Data Fig. 1). Because a shift towards healthier diets on a globally relevant scale is a complex and multifaceted challenge that is subject to various social, political and cultural barriers[22], we also assessed different levels of convergence towards healthier diets and compared the results with conservation actions in line with the targets of the Kunming-Montreal Global Biodiversity Framework (GBF)[23]. Our analysis differs from earlier studies that did not distinguish between different conservation value perspectives[14,21,24], only used simple aggregated biodiversity indicators[8,9,25,26], assessed the substitution of livestock food without considering further adjustments in food consumption[20,26] or lacked the integration of other environmental and socio-economic outcomes[21], and thus represents an important addition to the debate on diet-related benefits for nature.

The Model of Agricultural Production and its Impact on the Environment (MAgPIE, v4.8.2), a forward-looking open-source land and food-system model, formed the core of our modelling framework. MAgPIE is continually validated against observed data[27] and has frequently been used to study questions related to the sustainability of the food system[18,24]. It uses a wide range of socio-economic and spatially explicit biophysical information to simulate global land-system dynamics over the twenty-first century (see Methods). To map projected land-cover changes at a scale relevant for assessing fine-scale landscape and habitat change, we coupled MAgPIE with the Spatial Economic Allocation Landscape Simulator (SEALS). SEALS uses empirically calibrated adjacency relationships, physical suitability and conversion eligibility information to allocate projected land-cover changes at a spatial resolution of 10 arcsec (300 m × 300 m at the equator)[28,29].

Future scenarios of dietary change and conservation action

In our scenario set, we compared the effects of a partial and complete shift towards healthier diets with a bundle of conservation actions across the 'Nature for Nature' and 'Nature for Society' perspectives. Our reference scenario (SSP2-REF) follows the 'middle-of-the-road' shared socio-economic pathway (SSP2) for the land-use sector[30] with moderate population and income growth. In our reference scenario, we also assumed full compliance with currently implemented land policies, such as protected areas (PAs). In our alternative scenarios, we added a 50% (DIET50) and 100% (DIET100) convergence to a healthy reference diet by 2050 as outlined by the EAT-Lancet Commission[8], a set of targeted conservation measures to support biosphere integrity (BIOS) and lastly a combination of a partial diet shift and targeted conservation action (DIET50-BIOS) to the reference case.

The healthy reference diet is based on minimum daily per capita intakes of legumes, fruits, vegetables and nuts and maximum intakes of sugar, oils, poultry, eggs, red meat and dairy products, complemented by a convergence to a healthy body mass index (that is, 20–25)[7] (Fig. 1a). Within these limits, country-specific dietary patterns can still exhibit considerable diversity. Globally, the assumed partial (DIET50) and full (DIET100) convergence towards the healthy reference diet is associated with a reduction in average per capita calorie intake from livestock products of 33% and 66%, respectively, by 2050 (Fig. 1a). The reduction in livestock-based food intake is compensated by an increase in plant-based food intake, in particular from legumes (+173 and +346% kcal person^{-1} day^{-1}) and fruits, vegetables and nuts (+57 and +114% kcal person^{-1} day^{-1}).

In the BIOS scenario, we assessed land conservation measures in line with the GBF targets. These measures expand PAs to 30% of the global land surface and address key drivers of biodiversity loss outside of PAs. The assumed expansion of PAs includes unprotected land within Key Biodiversity Areas (KBAs)[31], intact habitat in Biodiversity Hotspots (BHs) and ecoregions with a high β-diversity (EBDs)[32], and critical connectivity areas (CCAs) as defined by Brennan et al.[13]. Conservation measures outside PAs include maintaining at least 20% of semi-natural habitats in agricultural landscapes[33,34] by 2030 and a no-net-biodiversity-loss scheme after 2030 whereby any decrease in biodiversity intactness[24] must be compensated at the biome level[35] (Methods).

More effective habitat conservation through targeted action

We estimated changes in the area of habitat (AOH) of vertebrate species based on a fine-scale allocation of land-cover projections and the corresponding changes in the suitable habitat within the range of each assessed species (Extended Data Table 1). AOH projections provide valuable information on potential habitat change and species extinction risk. They can also guide conservation efforts and have been proposed as an additional indicator for the International Union for Conservation of Nature (IUCN) Red List[36,37]. Although the number of species assessed (27,726) represents only around 2.2% of recorded species and 0.3% of all predicted species[38], the use of a large set of surrogate species across different taxa with varying traits and habitat preferences has shown to be effective in reproducing the spatial variation in biodiversity at national, regional or global scales[11,39]. In terms of conservation values, the AOH indicator is mostly associated with the 'Nature for Nature' value perspective.

In our reference scenario (SSP2-REF), we found that 17,359 (63%) of the assessed species could experience a combined global habitat loss of 22.5 Gha (Fig. 2). Of these species, 1,392 and 607 species could lose more than 20% and 40%, respectively, of their habitat by 2050, of which 60% are currently listed only as 'least concern' or 'near threatened' according to the IUCN Red List (Fig. 3). Much of this habitat loss is driven by the expansion of agricultural land in tropical Africa, Asia and Latin America (Supplementary Fig. 16) as a result of population growth and increasing per capita food supply, in particular of meat and dairy products owing to rising incomes (Extended Data Figs. 2–4). While in Latin America (LAM) and Asian countries excluding China, India and Japan (OAS) more than 80% of the habitat losses in SSP2-REF are due to further cropland expansion, nearly 40% of habitat losses in sub-Saharan Africa (SSA) are driven by pasture expansion (Fig. 2). In OAS, forest loss resulting from cropland and pasture expansion is particularly high, which especially affects forest-dwelling birds (Extended Data Figs. 5 and 6). In LAM and SSA, the loss of open ecosystems also significantly drives habitat loss in SSP2-REF, partly due to the relatively high baseline protection of forest compared with open ecosystems such as the Cerrado in Brazil (Supplementary Fig. 2). We also found that in Europe (EUR and NEU), China (CHA), as well as in Canada, Australia and New Zealand (CAZ), forest establishment in open ecosystems, for example due to land abandonment and rising timber demand, is a critical driver of habitat loss, further increasing the pressure on species adapted

 https://doi.org/10.1038/s41893-025-01595-9

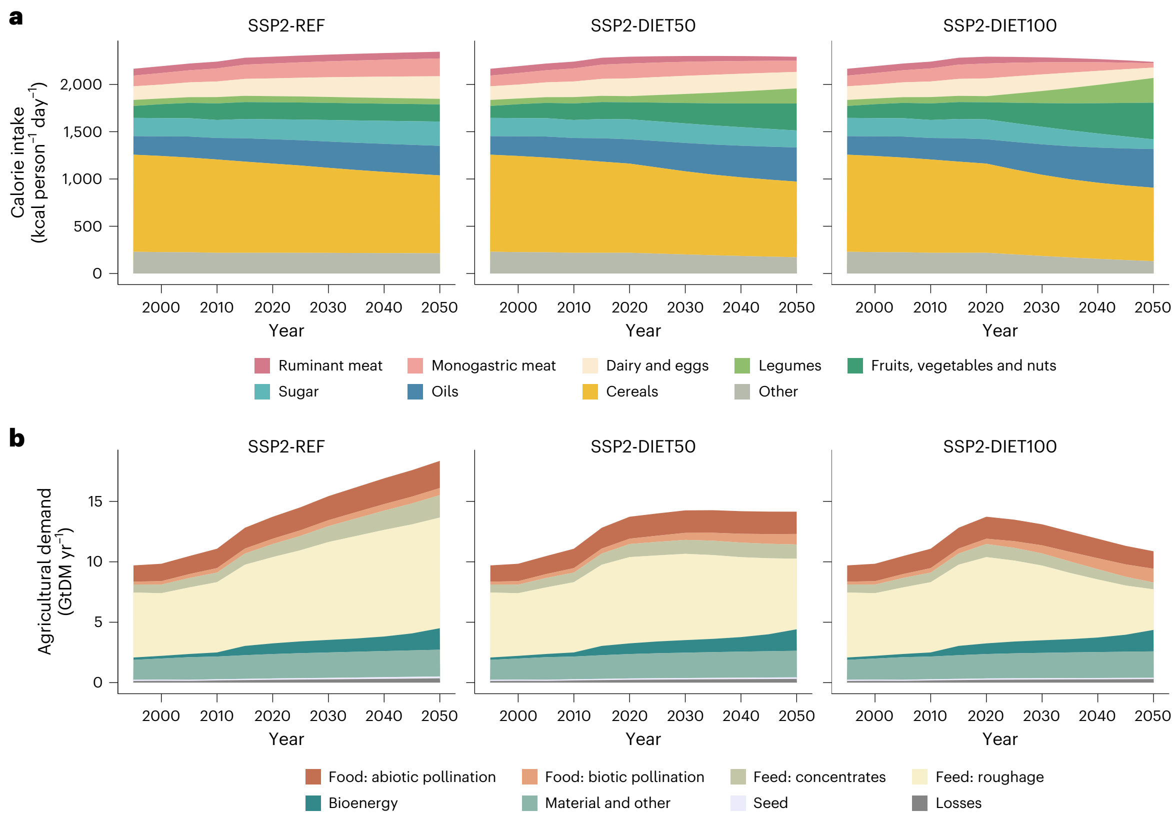

Fig. 1 | Global food consumption and agricultural demand in our dietary change scenarios. a, Per capita calorie intake per day across different food groups and for different levels of convergence towards recommended intake levels. In the reference scenario, calorie intake is derived from projected population growth, demographic changes and per capita income, while recommended intake levels in the two dietary change scenarios for the different food groups are based on Springmann et al.[7] (Methods). **b**, Overall changes in agricultural demand expressed in gigatonnes of dry matter (GtDM) per year for different levels of convergence towards the healthy reference diet across different demand categories. Food crops mediated by biotic pollination include oil crops such as sunflower or rapeseed, legumes, and fruits, vegetables and nuts.

to open habitats that have already experienced strong population declines over recent decades[40].

In our alternative scenarios, we found that compared with the SSP2-REF scenario, combined habitat loss is roughly halved in both the SSP2-DIET50 (−46%) and SSP2-DIET100 (−52%) cases (Fig. 2). This suggests only marginal benefits in terms of habitat loss are gained from full compared with partial convergence to the healthy reference diet, even though the reduction in global agricultural demand is almost twice as high in the SSP2-DIET100 scenario compared with in the SSP2-DIET50 scenario (Fig. 1). Similarly, the global number of species with a habitat loss ≥20% is also reduced by 60% across both diet change scenarios with almost no additional benefits from a complete transition to healthier diets (Fig. 3). In addition, and contrary to the global trend, we found that in SSA, the number of species with a habitat loss ≥20% and ≥40% actually increases in the SSP2-DIET100 scenario compared with in SSP2-REF (Extended Data Fig. 6) because land savings due to lower feed demand are offset by a shift from staple foods to other plant foods with a broader nutrient spectrum but a lower productivity per hectare, such as legumes or fruits, vegetables and nuts (Extended Data Fig. 4). By contrast, in LAM and OAS, the relative reductions in habitat loss (−84% and −78%, respectively) from even a partial dietary change compared with SSP2-REF are much higher than those observed at the global scale, suggesting disproportionate regional benefits in terms of habitat conservation resulting from a shift to more plant-based diets (Fig. 2).

However, our results also indicate that dietary change is not per se a prerequisite for habitat conservation as land conservation in line with the GBF exceeds the benefits of dietary change and drastically reduces habitat loss from food production. In particular, we found that the combined habitat loss in the SSP2-BIOS scenario is 77% and 51% lower compared with the SSP2-REF and SSP2-DIET100 scenarios, respectively (Fig. 2), even though agricultural demand is the same as in SSP2-REF. This also pertains to the number of species with ≥20% habitat loss, which is also 76% and 35% lower than in the SSP2-REF and SSP2-DIET100 scenarios, respectively. In SSA, we found that the conservation actions in our SSP2-BIOS scenario would reduce the number of species with ≥20% habitat loss by 70% and 71% compared with SSP2-REF and SSP2-DIET100, respectively (Extended Data Fig. 6). This indicates that habitat losses can be mitigated by stringent spatial planning that prevents land expansion in ecologically sensitive areas, even as agricultural demand increases. Despite a larger cropland area, especially for non-staple crops, we found no significant increase in the number of species with high habitat losses in the SSP2-DIET50-BIOS scenario compared with SSP2-BIOS (Extended Data Figs. 4 and 6), indicating that targeted conservation action better distributes impacts across space (Extended Data Fig. 7). Overall, these findings also hold against varying assumptions regarding socio-economic trends along the SSP1 (Sustainability) and SSP3 (Regional Rivalry) trajectories[30], although we found that, especially in SSA, cropland expansion in response to biosphere protection in the SSP1-BIOS scenario is larger because of greater trade liberalization (Supplementary Figs. 5–15).

Mixed outcomes of dietary shifts on NCP supply

Our analysis also includes indicators for the supply of key regulating NCP in cultured landscapes and climate regulation, which address the 'Nature for Society' conservation value perspective (Extended Data Table 1). These include changes in landscape pollination

Fig. 2 | AOH losses at global and regional levels between 2020 and 2050. a,**b**, Total sum of AOH losses at the global (**a**) and regional (**b**) levels between 2020 and 2050 caused by the expansion of aggregated land-use/land-cover (LULC) types across all assessed species.The sum of AOH losses is much higher than overall projected global and regional land-use changes. This is because one unit of expansion of each LULC type can cause loss of AOH for several species. Hence, the measure also indicates the relative importance of LULC expansions for AOH losses by putting a higher weight on areas that affect more species. The legend in **a** also applies to **b**. GLO, global; CAZ, Canada, Australia and New Zealand; CHA, China; EUR, European Union; IND, India; JPN, Japan; LAM, Latin America; MEA, Middle East and Northern Africa; NEU, non-EU European countries; OAS, other Asia; REF, reforming economies of the former Soviet Union; SSA, sub-Saharan Africa Note the different *x*-axis ranges across the regional plots.

sufficiency scores, which are an indicator for wild pollination supply, and configurational landscape heterogeneity. Configurational landscape heterogeneity has also shown to be positively associated with a range of other key regulating NCP, such as pest control, and is an important driver of biodiversity in managed landscapes[41,42]. We also used the Global Soil Erosion Modelling (GloSEM) platform to estimate changes in soil loss by water erosion, which is a dominant driver of degradation of soil-related NCP at the global scale[43,44]. Finally, we also report net CO_2 uptake and losses from land-use change for climate regulation and show how these affect total GHG emissions in the land sector (Extended Data Table 1).

Our data indicate that in 2020, the majority of cropland (970.6 Mha) was situated in landscapes with low configurational heterogeneity and pollination sufficiency scores. By 2050, declining

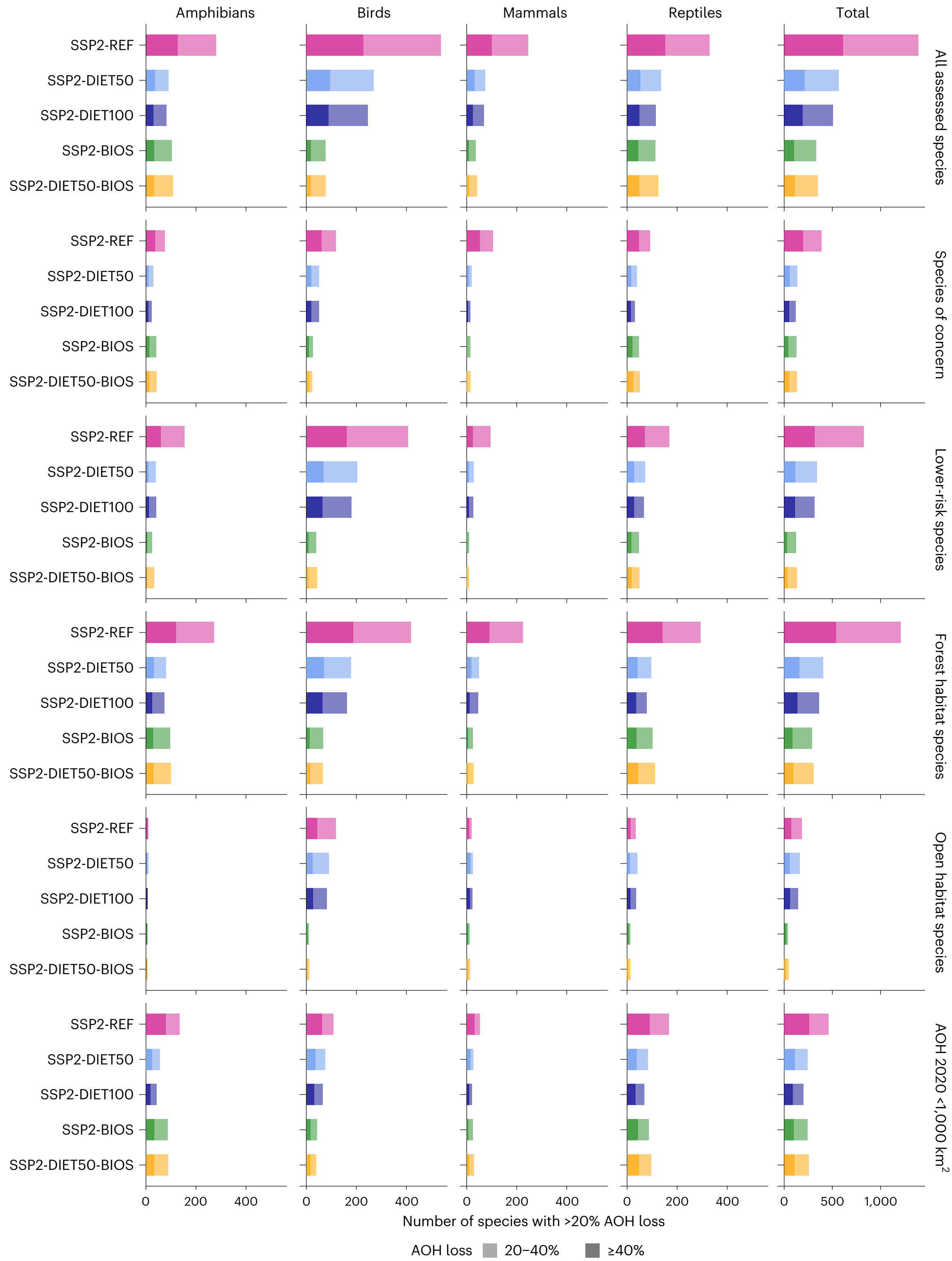

Fig. 3 | Species with more than 20% estimated AOH loss by 2050. Number of species with more than 20% estimated AOH loss by 2050 across modelled scenarios and different groupings. 'Species of concern' includes species that are currently 'vulnerable', 'endangered' and 'critically endangered' according to the IUCN Red List. 'Lower-risk species' includes species that are currently listed as 'least concern' or 'near threatened'.

landscape heterogeneity in SSP2-REF further increases the total cropland area with insufficient levels of wild pollination (Fig. 4b), particularly in SSA (+44.8 Mha), LAM (+11.4 Mha) and OAS (+34.6 Mha). This is notable because in SSP2-REF, the demand for pollinator-dependent food crops with a high nutritional value, such as fruits, vegetables, nuts, legumes and oil crops, also increases strongly in SSA (+167%), the Middle East and North Africa (MEA; +68%), OAS (+52%) and India (IND; +43%; Supplementary Fig. 17). In our diet change scenarios, the demand for pollinator-dependent food crops increases even further to 343% (DIET50) and 508% (DIET100) in SSA and 158% (DIET50) and 255% (DIET100) in OAS compared with today. Yet, despite some global improvements (Fig. 4b), we still found substantial increases in cropland

https://doi.org/10.1038/s41893-025-01595-9

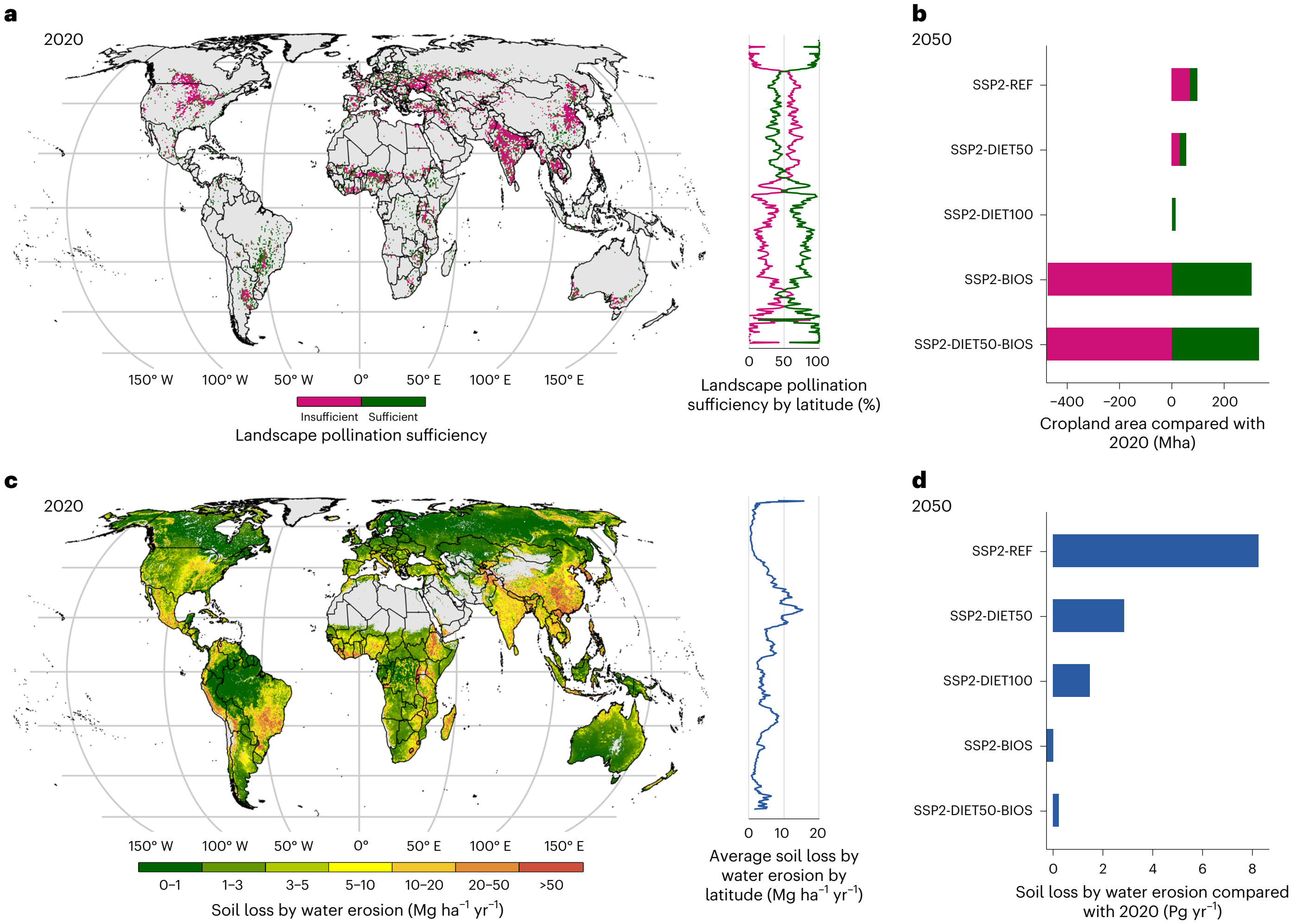

Fig. 4 | Landscape pollination sufficiency and soil loss by water erosion. **a**,**c**, Spatial (left) and latitudinal (right) estimates of landscape pollination sufficiency scores in total cropland (**a**) and soil loss by water erosion (**c**) for the reference year 2020. Spatial and latitudinal estimates for the year 2020 are directly derived from European Space Agency's Climate Change Initiative land-cover maps. Soil loss estimates are based on the GloSEM platform (Methods). Country polygons are adapted from ref. 100. **b**,**d**, Projected changes in landscape pollination sufficiency (**b**) and soil loss by water erosion (**d**) between 2020 and 2050 based on MAgPIE–SEALS land-cover projections. Continuous pollination sufficiency scores have been simplified into two categories of 'insufficient' (<1) and 'sufficient' (≥1) values. Basemaps in **a** and **c** adapted from World Bank Official Boundaries under a Creative Commons license CC BY 4.0.

area with insufficient levels of wild pollination, particularly in SSA (DIET50: +41.1 Mha; DIET100: +43.5 Mha) and to some extent in OAS (DIET50: +9.8 Mha; DIET100: +12.7 Mha; Extended Data Fig. 8). Maintaining at least 20% of semi-natural habitats at the landscape scale in SSP2-BIOS and SSP2-DIET50-BIOS, however, can address the structural trends that lead to cropland concentration, landscape simplification and reduced NCP supply (Fig. 4b and Extended Data Fig. 8).

In terms of soil loss by water erosion, we found that dietary change can effectively mitigate the high losses observed in SSP2-REF, mainly due to the smaller agricultural area in OAS and LAM, but also due to a higher share of perennial crops (Fig. 4d and Extended Data Fig. 9). However, again, we found only limited additional benefits of a complete dietary shift compared with a partial shift. By contrast, in SSA, we found no co-benefits of dietary change for soil loss by water erosion. However, as a result of production shifts to areas less prone to erosion, land conservation measures in the SSP2-BIOS and SSP2-DIET50-BIOS scenarios show significant co-benefits for soil loss in SSA, with soil loss lower by 1.1 Pg (BIOS) and 0.7 Pg (DIET50-BIOS) in 2050 compared with 2020, despite a larger cropland area.

In line with previous work[7,45], we also found significant co-benefits from dietary change both in terms of CO_2 emissions from land-use change and total GHG emissions from agriculture, forestry and other land use (AFOLU). Our results show that by 2050, a partial dietary shift (DIET50) can achieve more than three-quarters and almost two-thirds of the reductions in cumulative CO_2 and GHG emissions, respectively, of a full dietary shift (DIET100) compared with SSP2-REF (Fig. 5a,b). Furthermore, land conservation in our SSP2-BIOS scenario significantly increases carbon uptake on land (Fig. 5a and Supplementary Fig. 23). Reductions in total cumulative GHG emissions from land conservation are therefore similar to those achieved in SSP2-DIET50. The combination of GBF-aligned conservation with a partial dietary shift (DIET50-BIOS) even results in slightly lower cumulative GHG emissions than the SSP2-DIET100 scenario.

Furthermore, a decomposition of the contributions of the conservation measures in the SSP2-BIOS scenario shows that a simultaneous implementation of measures that address different conservation objectives is crucial to mitigate potential trade-offs between interventions. The no-net-loss scheme, however, caused notable benefits across all conservation value perspectives (Supplementary Figs. 31–35).

Partial dietary shift can lower barriers to conservation

We further complemented our analysis with additional indicators that provide an integrated perspective on changes in land productivity and food accessibility across our scenarios (Extended Data Table 1).

 https://doi.org/10.1038/s41893-025-01595-9

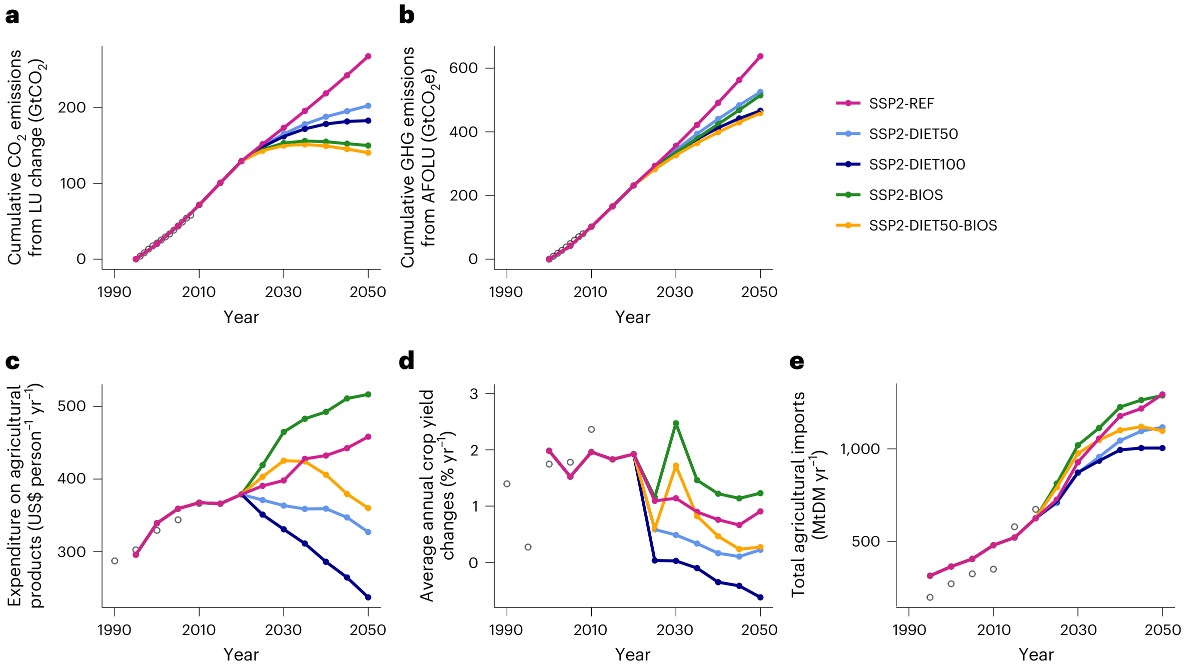

Fig. 5 | Global projections of GHG emissions from AFOLU, land productivity and food accessibility. a–e, Outcomes projected by MAgPIE for cumulative CO_2 emissions from land-use (LU) change (**a**), overall cumulative GHG emissions from AFOLU (**b**), expenditure on agricultural products for food use (**c**), average annual crop yield changes (**d**) and agricultural imports (**e**). Regional outcomes and sources of validation data (circles) are shown in Supplementary Figs. 21–30. $GtCO_2$, gigatonnes CO_2; $GtCO_2e$, gigatonnes CO_2-equivalent.

Our results show that targeted land conservation measures most consistently improve outcomes across both the 'Nature for Nature' and 'Nature for Society' conservation perspectives. However, we also found that compared with SSP2-REF, land conservation measures would incur notable additional socio-economic costs in terms of higher food expenditures (+13%), additional requirements for yield increases (+22.5% on average) and higher total agricultural imports (+3.5% globally between 2020 and 2050) if the demand trajectory remains unchanged (Fig. 5c–e). These higher costs would pose significant barriers to conservation action, particularly in LAM and many countries in OAS and SSA (Supplementary Figs. 26, 27 and 30). Yet, we crucially found that a partial convergence to healthier diets (SSP2-DIET50-BIOS) could largely offset these added barriers to conservation and would eventually result in lower food prices, required average yield increases and total imports compared with SSP2-REF.

Discussion

Our study provides several key learnings. First, our findings indicate that, across both the 'Nature for Nature' and 'Nature for Society' value perspectives, the added conservation benefits of a full dietary transition are modest compared with only a partial shift. This is because in regions of high global importance for conservation, such as Africa or Asia, converging towards healthier diets would mainly involve reducing the calorie supply of staple foods in favour of more diverse plant-based foods with a lower per hectare productivity rather than replacing resource-intensive livestock products as in most developed regions, and thus the marginal benefits of a complete dietary transition are limited. Secondly, GBF-aligned conservation action shows the most consistent conservation benefits, underlining the critical role of targeted land-use policies in decoupling conservation outcomes from food demand. Lastly, our results show that every step towards more plant-based diets would not only create strong co-benefits for GHG emissions but would also significantly reduce important socio-economic barriers to more effective conservation, such as higher food expenditure, agricultural intensification or increased imports.

In summary, we have shown that conservation across different value perspectives critically depends on proactive conservation action regardless of dietary patterns, but that the costs of conservation are significantly lower under a shift towards healthier diets.

Our analysis is an important addition to previous studies and provides further nuance to the debate on diet-related benefits across different conservation perspectives. In particular, the non-linear dynamics in our model results are not captured by static life cycle assessment approaches[10], trade analyses with input–output tables[9] or the use of biodiversity metrics that assign stylized biodiversity values to land-cover types[25,26]. Moreover, the high spatial granularity and dynamic representation of underlying socio-economic drivers, such as population and income growth or agricultural trade, were critical for understanding the consequences of dietary change across different regional contexts. In addition, our projections have shown to be robust to variations in key socio-economic assumptions, such as population and income growth, under the SSP1 and SSP3 scenarios (Supplementary Figs. 5–15).

While our study provides insights into the impacts of various land-system interventions on conservation outcomes, evaluating policy instruments to achieve the GBF targets or that support a transition to healthier diets was beyond the scope of the analysis. Achieving the GBF targets requires embedding nature conservation into cross-sector sustainable development programmes[46] to ensure reliable funding for implementation and monitoring[47], as well as addressing the distributional consequences of conservation actions[48]. The strong co-benefits of land conservation for both climate change mitigation and adaptation specifically imply an integration of policy approaches, such as redirecting carbon pricing revenues to ecosystem management programmes that prioritize the avoidance of habitat loss over offsets[49,50]. Although conservation action produces considerable benefits for society at large[29], local communities often face high costs that necessitate adequate compensation for foregone opportunities[51]. Furthermore, this study shows that some of the added costs of conservation can be avoided by a shift to healthier diets. Notable examples of strategies to alter dietary patterns include price-based interventions, information-based approaches and food environment policies[52]. Policy approaches that emphasize both human health and environmental benefits are likely to be the most effective[53]. This also includes improving economic access to food by addressing inequality[46], as 2.8 billion people, particularly in Africa and Asia, are currently unable to afford a healthy diet[54].

A critical component in our model framework is the link between modelled land-cover changes and the associations of species with habitat and elevation[55]. The MAgPIE model is systematically validated against historical data at the regional and global scale using a regularly updated validation database for most model outputs[27]. The SEALS downscaling model, in turn, is trained by using a loss function that evaluates modelled outputs against historic land-use patterns at high resolution[28,29]. The habitat–land-cover model[55] used here systematically reduces commission (false presence) errors and has shown to achieve high accuracies in AOH projections[56]. In reality, however, habitats are not only defined by biophysical land cover but by a complex interplay of various factors. Changes in habitat quality, for example through management[57], extraction[58] or pollution by nutrients or pesticides[59], could not be considered here. Higher input use efficiencies and improved management practices must accompany any yield increases to halt habitat degradation by pollution[7]. Climate change could also cause changes in the quality and distribution of suitable habitats[60] and may therefore interact with other drivers of habitat change[61]. Drastic reductions in GHG emissions and land-based carbon uptake through ecosystem restoration[28] are therefore critical to prevent climate-driven disruption of biodiversity[62], while adaptive conservation approaches need to consider habitat connectivity and the dispersal of species along environmental gradients[13,63].

Our study represents habitat and landscape change at a high spatial resolution within a dynamic framework. Yet, some socio-economic outcomes, such as price and endogenous yield changes, could only be derived at the scale of our model regions. Spatial variations in sub-regional food prices that would provide more detailed information on the distributional consequences of conservation due to the loss of opportunity or heterogeneity in market integration and access to infrastructure[64] were therefore not considered.

Our findings underline the global importance of coordinated and targeted action for nature conservation. This also involves reconciling diverse conservation value perspectives—including the 'Nature for Culture' perspective, which was not covered in our analysis—through active, informed deliberation among scientists, policymakers and the general public at local-to-global scales[65,66].

Methods

Model descriptions

MAgPIE. MAgPIE is a global, multi-regional land-system model for assessing global land-use dynamics and their implications for sustainable development in the twenty-first century[46,67]. It spatially allocates agricultural commodity production to meet global demand for food, feed, bioenergy and biomass under biophysical and socio-economic constraints based on a recursive dynamic cost-optimization approach. The model considers various cost components, such as factor requirements (capital, labour and fertilizer), land conversion, transport, investment in agricultural productivity and irrigation costs. The model also accounts for depreciation and new investments in capital stocks for crop production in each time step, favouring historically cultivated locations while limiting the unrestricted relocation of production to areas with favourable climatic conditions but with a lack of required infrastructure. Trade flows are split between historical import and export patterns and comparative advantages in production, including trade costs[68]. Spatially explicit biophysical information is derived from the dynamic global vegetation, crop and hydrology model LPJmL at a 0.5-degree spatial resolution based on historical climate data[69] (no climate change effects). Vegetation, litter and soil carbon stocks as well as water availability are taken from LPJmL4 (refs. 70,71), while crop irrigation water requirements and yield patterns (cropland and grassland) are derived from simulations with LPJmL5 with unlimited nitrogen supply[72]. To address computational constraints, all model inputs at 0.5-degree resolution are aggregated to spatial clusters for optimization using a *k*-means clustering algorithm[73]. Socio-economic constraints, such as trade patterns and interest rates, are defined at the scale of 12 model regions (Supplementary Fig. 1 and Supplementary Table 1), with larger economies resolved individually and smaller ones grouped together. All major crop and livestock species, non-food agricultural commodities and supply chain losses are included in MAgPIE. Land competition is modelled in terms of the cost-effectiveness between crop and livestock production, and considering the land conservation targets formulated in each scenario.

Following previous studies, several of the outcome indicators used here are directly derived from MAgPIE (Extended Data Table 1). Net CO_2 emissions from land-use change are calculated on the basis of carbon losses and uptake due to the conversion of forested and non-forest ecosystems and regrowth on abandoned agricultural land, respectively, between time steps[18]. CH_4 emissions include emissions from enteric fermentation, animal waste management, rice production and the burning of agricultural residues and are estimated from the level of ruminant livestock production, manure and area of rice production. N_2O emissions are estimated according to a nitrogen budget approach[74] that accounts for differences between organic and inorganic nitrogen inputs and removals through harvesting or grazing on agricultural land and also for differences between excreted and recycled manure in animal waste management. On non-agricultural land, we assume a stable state where nitrogen fixation equals surplus. Average annual crop yield changes are calculated from yield differences between time steps. Yield changes are driven by cropland relocation to areas with higher yields and the cost-effectiveness of investments into irrigation as well as research and development investments into yield-increasing technological change[75] compared with other cost components, such as land conversion or transport. Food prices are derived from the shadow price (Lagrange multiplier) of producing one additional unit of food and multiplied by the per capita supply of agricultural food products (including waste) to obtain the expenditure on agricultural products[76]. MAgPIE is intensely validated using the R library mrvalidation tool[27], which draws on a validation database that contains historical data for most output indicators (see also Supplementary Figs. 21–30).

SEALS. SEALS is used to map simulated land-cover changes in MAgPIE at a scale relevant for assessing landscape and biodiversity change[28,29] (see ref. 28 for a discussion of the MAgPIE–SEALS framework). SEALS spatially allocates projected land-cover changes from MAgPIE to a resolution of 10 arcsec (field scale) using adjacency relationships, physical suitability and conversion eligibility information. The initial state of the model landscape is defined by a high-resolution LULC map from the European Space Agency's Climate Change Initiative (ESA-CCI) for the year 2020. The 37 ESA-CCI land-cover classes are aggregated into 7 functional types, namely, cropland, grassland, forest, non-forest vegetation (for example, shrubland or herbaceous cover), urban, barren land and water. Subsequently, the spatial adjacency strength for each functional type on neighbouring land-cover pixels is quantified, considering both distance and pixel agglomeration. The physical suitability for land-cover allocation is determined by high-resolution data on soil type and quality, topographic information, climate and travel time to the nearest market. In addition, allocation constraints are applied to prevent further cropland or pasture expansion in areas such as urban land, current PAs or water bodies. In the BIOS scenario, the expansion of crop, pasture and urban land is also prohibited in conservation priority areas to meet the 30 × 30 target of the GBF (see below). The overall suitability map is formed by combining adjacency relations, physical suitability and conversion eligibility, where pixels are ranked according to their suitability. In an iterative process, land-cover changes are then allocated to the highest-ranked grid cells until all projected changes from MAgPIE between 2020 and 2050 are assigned to generate high-resolution land-cover maps for each modelled scenario. Specific coefficients for different adjacency relationships and physical suitability are empirically determined by iteratively applying the allocation algorithm on a time series (2000–2010) of LULC maps from ESA-CCI. The coefficients most predictive on withheld historical data (2011–2015) are selected during this process[28,29].

Biodiversity and NCP indicators

Landscape pollination sufficiency. Changes in configurational landscape heterogeneity and pollination sufficiency were derived on the basis of fine-scale projections (300 m × 300 m at the equator) of land-cover changes using MAgPIE–SEALS coupling. Pollination sufficiency is defined by the presence of semi-natural habitat (native forest and non-forest vegetation, including native grassland) near cropland[28,77]. To derive pollination sufficiency scores, we ranked all cropland pixels from 0 to 1 based on the proportion of semi-natural habitat within a 2-km foraging radius typically found in wild pollinator communities. We assigned a value of 1 where the proportion of semi-natural habitat within the foraging range around cropland is >30%, while values between 0 and 1 indicate a proportion of 0–30% (refs. 28,78). Although this metric does not account for other important factors that affect wild pollinator abundance, such as pesticide applications, the presence of meta populations, or the quality of nesting habitats or floral resources, multiple global and local studies have shown that the amount of semi-natural habitat around cropland can function both as a reliable proxy for wild pollination supply and as an important driver of biodiversity and other regulating NCP in various landscape contexts[41,79].

Soil loss by water erosion. Soil loss by water erosion was estimated using the GloSEM platform. GloSEM uses a global geographical information system (GIS) implementation of the Revised Universal Soil Loss Equation (RUSLE) model, which was developed and validated by Borelli et al.[4,44]. In contrast to process-based soil erosion models, which have limited global applicability, GloSEM uses a parsimonious yet physically plausible approach to quantify soil erosion resulting from sheet and drill erosion processes at field scale. The accuracy of soil loss estimates from RUSLE-type models such as GloSEM has demonstrated to be suitable for most practical and policy applications[44]. Similar to other RUSLE-type models, soil loss in GloSEM is determined by a driving force (rainfall erosivity), a resistance term (erodibility of the soil) as well as topographical and land-cover information. Global rainfall erosivity maps were derived from the Global Rainfall Erosivity Database using Gaussian process regression and covariates from the WorldClim database[80], while soil erodibility was estimated using soil data from the International Soil Reference and Information Centre (ISRIC) SoilGrids database[81]. Topographical information was obtained by processing digital elevation model (DEM) data using a two-dimensional GIS-based approach[82]. The land-cover and management factor was calculated using separate approaches for cropland and non-cropland areas. For cropland, spatial cropping patterns from MAgPIE at the 0.5-degree level were used and individual land-cover factors were assigned to 20 crop functional types based on literature values[44]. Subsequently, an area-weighted mean between all crop groups in each 0.5-degree grid cell was calculated and matched to projected fine-scale cropland maps from MAgPIE–SEALS. In non-cropland areas, land-cover factors were estimated by combining literature values for forested and non-forested areas with potential annual vegetation and forest-cover maps based on FCOVER data[83] and tree-cover data[84], as detailed in von Jeetze et al.[28].

Area of habitat. The AOH refers to the habitat available to a species within its geographic range[37]. Here, we produced vertebrate AOH maps for 6,374 amphibian, 9,124 bird, 5,351 mammal and 6,877 reptile species for the year 2020 and used land-cover projections based on the MAgPIE–SEALS framework to assess AOH changes under different land-use scenarios. Range polygons for each species were obtained from the IUCN Red List[85] and BirdLife International[86]. In line with previous work, we retained separate range polygons for resident, breeding, non-breeding and uncertain seasonality during processing[11,36], but aggregated the final results across all seasonal ranges of each species to simplify the presentation of our results. We further excluded all species ranges with unknown presence and species with no habitat information. Habitat preferences for each species were derived from the IUCN Red List[85] and are reported for 12 different habitat classes based on the IUCN Habitats Classification Scheme[87]. To relate the IUCN habitats to spatial land-cover information we used the habitat–land cover model of Lumbierres et al.[55]. The model associates 12 main habitat classes of the IUCN Habitats Classification Scheme with ESA-CCI land-cover classes and provides a translation table based on 3 different thresholds of positive association. We selected the threshold with the strongest habitat–land-cover association, which in similar applications has shown to considerably reduce commission errors without compromising validation performance of the AOH estimates[36,56]. For artificial degraded forest and plantation habitats, we chose the second strongest association threshold because none of the association values surpassed the threshold with the strongest association. Artificial degraded forest and plantation habitats were therefore associated with ESA-CCI classes 12 (cropland, rainfed, tree or shrub cover), 20 (cropland, irrigated or post-flooding) and 190 (urban areas[55]; see Supplementary Table 2). Habitats classified as marginal or of no major importance in the IUCN Red List were omitted from the data. For abandoned agricultural land we followed the approach of Humpenöder et al.[88] with updated parameters for the Chapman–Richards growth function from Braakhekke et al.[89], which assumes the same carbon density and the same species pool as during natural succession. Thus, in the early stages of natural succession, when the carbon density is ≤20 tC ha^{-1}, the land is classified as non-forest vegetation (native grassland or shrubland) in the 'other land' pool. After reaching a carbon density of >20 tC ha^{-1}, the land is classified as forest vegetation. We maintained this approach in the MAgPIE–SEALS coupling and classified abandoned agricultural land in the early successional stage as open habitat (native grassland or shrubland) and land in the later successional stages as forest habitat.

Changes in AOH were estimated following a two-step approach involving a pre-processing step and a scenario processing step (Supplementary Fig. 3). The pre-processing step involved subtracting unsuitable elevation areas from the range[37] and translating IUCN habitats to ESA-CCI land-cover classes for each species. Species elevational range data were also obtained from the IUCN Red List and areas outside the elevational limits were subtracted on the basis of WorldClim 1-km elevation data[90]. Some range polygons had no remaining areas within their species elevational limits and were therefore omitted from the dataset. During the scenario processing step, unsuitable areas were subtracted from the pre-processed range polygons based on habitat preferences and land-cover projections from MAgPIE–SEALS to produce the final AOH estimates. AOH estimates for the year 2020 were derived directly from the ESA-CCI land-cover map. All calculations were performed using R (ref. 91) and the terra package[92]. Owing to the high computational load, computations were run on a high-performance cluster and parallelized using the packages foreach[93] and doParallel[93].

Modelled scenarios

We used the 'middle-of-the-road' socio-economic pathway (SSP2) for the land-use sector[30] as our reference scenario. The SSP2 pathway assumes continued trends of moderate population and income growth and includes currently implemented land-use regulations.

Ensuing food demand projections are based on anthropometric and econometric approaches that incorporate country-specific information on income, body-height, age-cohort, sex and body-mass-index distributions with elasticity parameters derived from historical data[6]. Information on PAs in the historical period (1995–2020) was taken from the World Database on Protected Areas (WDPA)[94]. We selected all legally protected areas that meet the IUCN and Convention on Biological Diversity definitions of PAs. Land use within PAs was determined on the basis of ESA-CCI land-cover data and aggregated to MAgPIE land pools. In the reference scenario, land use within PAs after 2020 was held constant (that is, no cropland, pasture or urban expansion), assuming full compliance and considering mixed land use, such as in IUCN PA categories V and VI.

Our alternative scenarios differ from the reference scenario in terms of per capita food demand multiplied by the projected total population, as we assume a 50% (DIET50) and 100% (DIET100) convergence towards healthier diets, and the implementation of biodiversity conservation measures (BIOS) at the global scale.

- DIET50 and DIET100: the healthy reference diet is based on minimum and maximum recommended daily intakes for different food groups, while allowing for considerable diversity in country-specific dietary patterns within the ranges of the recommended intake levels[7]. Minimum per capita intakes are formulated for legumes, fruits, vegetables and nuts. In countries where per capita intakes of these food groups do not meet the recommended levels, intakes are increased to these minimum levels. Maximum intakes are set for sugar, oils, poultry, eggs, red meat and dairy products. Where per capita intakes exceed the recommended amounts, intakes of these food groups are reduced to meet the recommendations. In addition, a convergence towards a healthy body mass index of 20 to 25 is assumed. The food-specific maximum and minimum intakes for the healthy reference diet were derived from Springmann et al.[7], who have already considered country-specific dietary patterns. In the DIET100 scenario, we assume a full linear convergence towards the recommended dietary intakes by 2050. In the DIET50 scenario, we assume only a 50% convergence towards the per capita intake targets of the healthy reference diet. These are then linearly combined with the reference food intake following the SSP2 trajectory (Fig. 1). In terms of total daily calorie intake, we also assume a 50% convergence from the reference total calorie intake level to the total calorie target level, which is informed by the healthy body mass index target (20–25). However, to maintain minimum and maximum targets for the different food items of the healthy reference diet, we only adjusted the intake of staple calories to meet the total calorie targets.
- BIOS: the BIOS scenario includes a bundle of conservation measures to support biosphere integrity. Compared with the reference scenario, the area of protected land is increased by 2,055 Mha to meet the GBF target of conserving at least 30% of the global land surface by 2030. The enlargement of protected areas is focused on areas of global importance for biodiversity conservation (Supplementary Fig. 2), including KBAs[31], unprotected habitat in BHs and EBDs[32], as well as the CCAs identified by Brennan et al.[13]. Our choice to expand protected areas in KBAs, BHs, EBDs and CCAs is informed by the current literature on conservation priority areas and seeks to balance different conservation objectives, taking into account areas of global importance as well as species migration[13,32]. Yet it remains just one plausible implementation of the GBF 30 × 30 target aimed at illustrating how land protection could contribute to global conservation. We assume that within these conservation priority areas, restoration targets for different land-cover types are based on pre-industrial (1750) levels derived from the LUH2 (v2) dataset[95]. In addition, the BIOS scenario also includes a set of measures that address key drivers of biodiversity loss outside of PAs. These include maintaining at least 20% of semi-natural vegetation (SNV) in managed landscapes by 2030 and a no-net-biodiversity-loss scheme after 2030 at the biome level[35]. The constraint to maintain at least 20% of SNV (native forest and non-forest vegetation) in managed landscapes is directly applied in the MAgPIE model and is formulated such that 20% of the potentially available cropland must be reserved for SNV. Because evidence suggests that the 20% target should be fulfilled at the 1 km × 1 km scale to achieve maximum benefits[33,34], we also used high-resolution satellite imagery from the Copernicus Global Land Service[96] to estimate how much current cropland would need to be relocated to other areas to fulfil this target. This information is then used as additional input in the model optimization. Furthermore, the constraint to maintain 20% SNV at the 1 km × 1 km level is also applied during the land allocation at high resolution with SEALS. Because SEALS uses a latitude/longitude World Geodetic System 1984 coordinate reference system (CRS), where the area covered by a single pixel varies with latitude, we used an Eckert IV equal-area CRS to identify which pixels should be conserved to maintain 20% SNV at the 1 km × 1 km scale and reprojected them to the latitude/longitude CRS. The no-net-biodiversity-loss scheme prohibits any reduction in the Biodiversity Intactness Index[24] (BII) of each biome[35] within a MAgPIE region and biogeographic realm. Any decrease in the area-weighted average BII at the biome level (for example, due to cropland or urban expansion) must therefore be offset by an increase in land uses with higher BII values within the same biome. The no-net-loss scheme thus acts as an additional guardrail for areas outside conservation priority areas and disincentivizes avoidable land conversions to agricultural land use. MAgPIE-specific BII coefficients for different land-use classes are based on Leclère et al.[24] and are presented in Supplementary Table 3.

Reporting summary

Further information on research design is available in the Nature Portfolio Reporting Summary linked to this article.

Data availability

The model results presented in this Article are available via Zenodo at https://doi.org/10.5281/zenodo.10599895 (ref. 97).

Code availability

The model code of the MAgPIE model is openly available under GNU Affero General Public License, version 3 (AGPLv3), and is accessible via GitHub at https://github.com/magpiemodel/magpie. The release version (MAgPIE 4.8.2) on which this work is based is available via Zenodo at https://doi.org/10.5281/zenodo.13833444 (ref. 98). MAgPIE 4.8.2 is accompanied by technical model documentation (https://rse.pik-potsdam.de/doc/magpie/4.8.2/), which was compiled using the GAMS code documentation toolkit goxygen[99]. The SEALS code is also accessible via GitHub at https://github.com/jandrewjohnson/seals_dev/releases/tag/v1.0.0 and the accompanying documention is available at https://justinandrewjohnson.com/earth_economy_devstack/seals_overview.html.

References

1. Matson, P. A., Parton, W. J., Power, A. G. & Swift, M. J. Agricultural intensification and ecosystem properties. *Science* **277**, 504–509 (1997).
2. *Global Assessment Report on Biodiversity and Ecosystem Services of the Intergovernmental Science-Policy Platform on Biodiversity and Ecosystem Services* (IPBES, 2019).

3. Poore, J. & Nemecek, T. Reducing food's environmental impacts through producers and consumers. *Science* **360**, 987–992 (2018).
4. Borrelli, P. et al. An assessment of the global impact of 21st century land use change on soil erosion. *Nat. Commun.* **8**, 2013 (2017).
5. Crippa, M. et al. Food systems are responsible for a third of global anthropogenic GHG emissions. *Nat. Food* **2**, 198–209 (2021).
6. Bodirsky, B. L. et al. The ongoing nutrition transition thwarts long-term targets for food security, public health and environmental protection. *Sci. Rep.* **10**, 19778 (2020).
7. Springmann, M. et al. Options for keeping the food system within environmental limits. *Nature* **562**, 519–525 (2018).
8. Willett, W. et al. Food in the Anthropocene: the EAT–Lancet Commission on healthy diets from sustainable food systems. *Lancet* **393**, 447–492 (2019).
9. Read, Q. D., Hondula, K. L. & Muth, M. K. Biodiversity effects of food system sustainability actions from farm to fork. *Proc. Natl Acad. Sci. USA* **119**, e2113884119 (2022).
10. Scarborough, P. et al. Vegans, vegetarians, fish-eaters and meat-eaters in the UK show discrepant environmental impacts. *Nat. Food* **4**, 565–574 (2023).
11. Jung, M. et al. Areas of global importance for conserving terrestrial biodiversity, carbon and water. *Nat. Ecol. Evol.* **5**, 1499–1509 (2021).
12. Fisher, B., Turner, R. K. & Morling, P. Defining and classifying ecosystem services for decision making. *Ecol. Econ.* **68**, 643–653 (2009).
13. Brennan, A. et al. Functional connectivity of the world's protected areas. *Science* **376**, 1101–1104 (2022).
14. Rasche, L., Habel, J. C., Stork, N., Schmid, E. & Schneider, U. A. Food versus wildlife: will biodiversity hotspots benefit from healthier diets? *Glob. Ecol. Biogeogr.* **31**, 1090–1103 (2022).
15. Poschlod, P. & Braun-Reichert, R. Small natural features with large ecological roles in ancient agricultural landscapes of Central Europe—history, value, status, and conservation. *Biol. Conserv.* **211**, 60–68 (2017).
16. Klasen, S. et al. Economic and ecological trade-offs of agricultural specialization at different spatial scales. *Ecol. Econ.* **122**, 111–120 (2016).
17. Coomes, O. T., Barham, B. L., MacDonald, G. K., Ramankutty, N. & Chavas, J.-P. Leveraging total factor productivity growth for sustainable and resilient farming. *Nat. Sustain.* **2**, 22–28 (2019).
18. Humpenöder, F. et al. Projected environmental benefits of replacing beef with microbial protein. *Nature* **605**, 90–96 (2022).
19. Kim, H. et al. Towards a better future for biodiversity and people: modelling Nature Futures. *Glob. Environ. Change* **82**, 102681 (2023).
20. Henry, R. C. et al. The role of global dietary transitions for safeguarding biodiversity. *Glob. Environ. Change* **58**, 101956 (2019).
21. Williams, D. R. et al. Proactive conservation to prevent habitat losses to agricultural expansion. *Nat. Sustain.* **4**, 314–322 (2021).
22. Fehér, A., Gazdecki, M., Véha, M., Szakály, M. & Szakály, Z. A comprehensive review of the benefits of and the barriers to the switch to a plant-based diet. *Sustainability* **12**, 4136 (2020).
23. *Kunming-Montreal Global Biodiversity Framework* CBD/COP/15/L25 (Convention on Biological Diversity, 2022); https://www.cbd.int/doc/c/3119/8611/72d7962a5b058cc30e2299c7/cop-15-17-en.pdf
24. Leclère, D. et al. Bending the curve of terrestrial biodiversity needs an integrated strategy. *Nature* **585**, 551–556 (2020).
25. Marquardt, S. G. et al. Identifying regional drivers of future land-based biodiversity footprints. *Glob. Environ. Change* **69**, 102304 (2021).
26. Kozicka, M. et al. Feeding climate and biodiversity goals with novel plant-based meat and milk alternatives. *Nat. Commun.* **14**, 5316 (2023).
27. Bodirsky, B. L. et al. mrvalidation: madrat data preparation for validation purposes. *Zenodo* https://doi.org/10.5281/ZENODO.7234083 (2024).
28. von Jeetze, P. J. et al. Projected landscape-scale repercussions of global action for climate and biodiversity protection. *Nat. Commun.* **14**, 2515 (2023).
29. Johnson, J. A. et al. Investing in nature can improve equity and economic returns. *Proc. Natl Acad. Sci. USA* **120**, e2220401120 (2023).
30. Popp, A. et al. Land-use futures in the shared socio-economic pathways. *Glob. Environ. Change* **42**, 331–345 (2017).
31. Birdlife International *World Database of Key Biodiversity Areas* (KBA Partnership, 2022); http://keybiodiversityareas.org/kba-data/request
32. Dinerstein, E. et al. A "Global Safety Net" to reverse biodiversity loss and stabilize Earth's climate. *Sci. Adv.* **6**, eabb2824 (2020).
33. Rockström, J. et al. Safe and just Earth system boundaries. *Nature* **619**, 102–111 (2023).
34. Garibaldi, L. A. et al. Working landscapes need at least 20% native habitat. *Conserv. Lett.* **14**, e12773 (2020).
35. Olson, D. M. et al. Terrestrial ecoregions of the world: a new map of life on Earth: a new global map of terrestrial ecoregions provides an innovative tool for conserving biodiversity. *BioScience* **51**, 933–938 (2001).
36. Lumbierres, M. et al. Area of habitat maps for the world's terrestrial birds and mammals. *Sci. Data* **9**, 749 (2022).
37. Brooks, T. M. et al. Measuring terrestrial area of habitat (AOH) and its utility for the IUCN Red List. *Trends Ecol. Evol.* **34**, 977–986 (2019).
38. Mora, C., Tittensor, D. P., Adl, S., Simpson, A. G. B. & Worm, B. How many species are there on Earth and in the ocean? *PLoS Biol.* **9**, e1001127 (2011).
39. Tälle, M., Ranius, T. & Öckinger, E. The usefulness of surrogates in biodiversity conservation: ` synthesis. *Biol. Conserv.* **288**, 110384 (2023).
40. Burns, F. et al. Abundance decline in the avifauna of the European Union reveals cross-continental similarities in biodiversity change. *Ecol. Evol.* **11**, 16647–16660 (2021).
41. Estrada-Carmona, N., Sánchez, A. C., Remans, R. & Jones, S. K. Complex agricultural landscapes host more biodiversity than simple ones: ` global meta-analysis. *Proc. Natl Acad. Sci. USA* **119**, e2203385119 (2022).
42. Tscharntke, T., Grass, I., Wanger, T. C., Westphal, C. & Batáry, P. Beyond organic farming–harnessing biodiversity-friendly landscapes. *Trends Ecol. Evol.* **36**, 919–930 (2021).
43. Vereecken, H. et al. Modeling soil processes: review, key challenges, and new perspectives. *Vadose Zone J.* **15**, 1–57 (2016).
44. Borrelli, P. et al. Land use and climate change impacts on global soil erosion by water (2015–2070). *Proc. Natl Acad. Sci. USA* **117**, 21994–22001 (2020).
45. Humpenöder, F. et al. Food matters: dietary shifts increase the feasibility of 1.5 °C pathways in line with the Paris Agreement. *Sci. Adv.* **10**, eadj3832 (2024).
46. Soergel, B. et al. A sustainable development pathway for climate action within the UN 2030 Agenda. *Nat. Clim. Change* **11**, 656–664 (2021).
47. Hughes, A. C. The Post-2020 Global Biodiversity Framework: how did we get here, and where do we go next? *Integr. Conserv.* **2**, 1–9 (2023).
48. Armstrong, C. Global justice and the opportunity costs of conservation. *Conserv. Biol.* **37**, e14018 (2023).
49. Barbier, E. B., Lozano, R., Rodríguez, C. M. & Troëng, S. Adopt a carbon tax to protect tropical forests. *Nature* **578**, 213–216 (2020).
50. Maron, M. et al. 'Nature positive' must incorporate, not undermine, the mitigation hierarchy. *Nat. Ecol. Evol.* **8**, 14–17 (2024).

51. Green, J. M. H. et al. Local costs of conservation exceed those borne by the global majority. *Glob. Ecol. Conserv.* **14**, e00385 (2018).
52. Gaupp, F. et al. Food system development pathways for healthy, nature-positive and inclusive food systems. *Nat. Food* **2**, 928–934 (2021).
53. Temme, E. H. M. et al. Demand-side food policies for public and planetary health. *Sustainability* **12**, 5924 (2020).
54. *The State of Food Security and Nutrition in the World 2024* (FAO, IFAD, UNICEF, WFP and WHO, 2024); https://doi.org/10.4060/cd1254en
55. Lumbierres, M. et al. Translating habitat class to land cover to map area of habitat of terrestrial vertebrates. *Conserv. Biol.* **36**, e13851 (2022).
56. Dahal, P. R., Lumbierres, M., Butchart, S. H. M., Donald, P. F. & Rondinini, C. A validation standard for area of habitat maps for terrestrial birds and mammals. *Geosci. Model Dev.* **15**, 5093–5105 (2022).
57. Ernst, R. et al. A frog's eye view: logging roads buffer against further diversity loss. *Front. Ecol. Environ.* **14**, 353–355 (2016).
58. Benítez-López, A. et al. The impact of hunting on tropical mammal and bird populations. *Science* **356**, 180–183 (2017).
59. Sánchez-Bayo, F. & Wyckhuys, K. A. G. Worldwide decline of the entomofauna: a review of its drivers. *Biol. Conserv.* **232**, 8–27 (2019).
60. *Scientific Outcome of the IPBES-IPCC Co-Sponsored Workshop on Biodiversity and Climate Change* (IPBES and IPCC, 2021).
61. Foden, W. B. et al. Identifying the world's most climate change vulnerable apecies: a systematic trait-based assessment of all birds, amphibians and corals. *PLoS ONE* **8**, e65427 (2013).
62. Trisos, C. H., Merow, C. & Pigot, A. L. The projected timing of abrupt ecological disruption from climate change. *Nature* **580**, 496–501 (2020).
63. Beger, M. et al. Demystifying ecological connectivity for actionable spatial conservation planning. *Trends Ecol. Evol.* **37**, 1079–1091 (2022).
64. Cedrez, C. B., Chamberlin, J. & Hijmans, R. J. Seasonal, annual, and spatial variation in cereal prices in sub-Saharan Africa. *Glob. Food Sec.* **26**, 100438 (2020).
65. Pascual, U. et al. Biodiversity and the challenge of pluralism. *Nat. Sustain.* **4**, 567–572 (2021).
66. Berkes, F. Community-based conservation in a globalized world. *Proc. Natl Acad. Sci. USA* **104**, 15188–15193 (2007).
67. Weindl, I. et al. Food and land system transformations under different societal perspectives on sustainable development. *Environ. Res. Lett.* **19**, 124085 (2024).
68. Schmitz, C. et al. Trading more food: implications for land use, greenhouse gas emissions, and the food system. *Glob. Environ. Change* **22**, 189–209 (2012).
69. Mengel, M., Treu, S., Lange, S. & Frieler, K. ATTRICI v1.1—counterfactual climate for impact attribution. *Geosci. Model Dev.* **14**, 5269–5284 (2021).
70. Schaphoff, S. et al. LPJmL4—a dynamic global vegetation model with managed land—part 1: model description. *Geosci. Model Dev.* **11**, 1343–1375 (2018).
71. Schaphoff, S. et al. LPJmL4—a dynamic global vegetation model with managed land—part 2: model evaluation. *Geosci. Model Dev.* **11**, 1377–1403 (2018).
72. von Bloh, W. et al. Implementing the nitrogen cycle into the dynamic global vegetation, hydrology, and crop growth model LPJmL (version 5.0). *Geosci. Model Dev.* **11**, 2789–2812 (2018).
73. Dietrich, J. P., Popp, A. & Lotze-Campen, H. Reducing the loss of information and gaining accuracy with clustering methods in a global land-use model. *Ecol. Modell.* **263**, 233–243 (2013).
74. Bodirsky, B. L. et al. N_2O emissions from the global agricultural nitrogen cycle—current state and future scenarios. *Biogeosciences* **9**, 4169–4197 (2012).
75. Dietrich, J. P., Schmitz, C., Lotze-Campen, H., Popp, A. & Müller, C. Forecasting technological change in agriculture—an endogenous implementation in a global land use model. *Technol. Forecast. Soc. Change* **81**, 236–249 (2014).
76. Stevanović, M. et al. Mitigation strategies for greenhouse gas emissions from agriculture and land-use change: consequences for food prices. *Environ. Sci. Technol.* **51**, 365–374 (2017).
77. Chaplin-Kramer, R. et al. Global modeling of nature's contributions to people. *Science* **366**, 255–258 (2019).
78. Kremen, C., Williams, N. M., Bugg, R. L., Fay, J. P. & Thorp, R. W. The area requirements of an ecosystem service: crop pollination by native bee communities in California. *Ecol. Lett.* **7**, 1109–1119 (2004).
79. Dainese, M. et al. A global synthesis reveals biodiversity-mediated benefits for crop production. *Sci. Adv.* **5**, eaax0121 (2019).
80. Panagos, P. et al. Global rainfall erosivity assessment based on high-temporal resolution rainfall records. *Sci. Rep.* **7**, 4175 (2017).
81. Hengl, T. et al. SoilGrids1km—global soil information based on automated mapping. *PLoS ONE* **9**, e105992 (2014).
82. Desmet, P. J. J. & Govers, G. A GIS procedure for automatically calculating the USLE LS factor on topographically complex landscape units. *J. Soil Water Conserv.* **51**, 427–433 (1996).
83. Fuster, B. et al. Quality assessment of PROBA-V LAI, fAPAR and fCOVER collection 300 m products of Copernicus Global Land Service. *Remote Sens.* **12**, 1017 (2020).
84. Hansen, M. C. et al. High-resolution global maps of 21st-century forest cover change. *Science* **342**, 850–853 (2013).
85. *The IUCN Red List of Threatened Species. Version 2020-2*. (IUCN, accessed 25 November 2020); https://www.iucnredlist.org
86. . *Bird Species Distribution Maps of the World* Version 2020.1 (BirdLife International and Handbook of the Birds of the World, accessed 26 February 2021); http://datazone.birdlife.org/species/requestdis
87. *Habitats Classification Scheme* Version 3.1 (IUCN, 2012).
88. Humpenöder, F. et al. Investigating afforestation and bioenergy CCS as climate change mitigation strategies. *Environ. Res. Lett.* **9**, 064029 (2014).
89. Braakhekke, M. C. et al. Modeling forest plantations for carbon uptake with the LPJmL dynamic global vegetation model. *Earth Syst. Dyn.* **10**, 617–630 (2019).
90. Fick, S. E. & Hijmans, R. J. WorldClim 2: new 1-km spatial resolution climate surfaces for global land areas. *Int. J. Climatol.* **37**, 4302–4315 (2017).
91. R Core Team. R: A language and environment for statistical computing. Version 4.3.2. (2023).
92. Hijmans, R. J. terra: Spatial data analysis. Version 1.7.55 https://rspatial.org/terra/ (2023).
93. Microsoft Corporation & Weston, S. doParallel: Foreach parallel adaptor for the 'parallel' package. Version 1.0.17 https://CRAN.R-project.org/package=doParallel (2023).
94. *The World Database on Protected Areas* (UNEP-WCMC and IUCN, accessed 23 March 2022); www.protectedplanet.net
95. Hurtt, G. C. et al. Harmonization of global land use change and management for the period 850–2100 (LUH2) for CMIP6. *Geosci. Model Dev.* **13**, 5425–5464 (2020).
96. Buchhorn, M. et al. Copernicus global land service: land cover 100m: collection 3: epoch 2019: globe. *Zenodo* https://doi.org/10.5281/zenodo.3939050 (2020).
97. von Jeetze, P. et al. Conservation outcomes of dietary transitions across different values of nature—model outputs. *Zenodo* https://doi.org/10.5281/zenodo.10599895 (2025).

98. Dietrich, J. P. et al. MAgPIE—an open source land-use modeling framework. *Zenodo* https://doi.org/10.5281/zenodo.13833444 (2025).
99. Dietrich, J. P., Kristine, K., David, K. & Lavinia, B. goxygen: in-code documentation for GAMS. *Zenodo* https://doi.org/10.5281/ZENODO.3909376 (2020).
100. World Bank Official Boundaries (World Bank, 2022); https://datacatalog.worldbank.org/search/dataset/0038272/World-Bank-Official-Boundaries

Acknowledgements

This work received funding from the European Union's Horizon Europe Research and Innovation programme (grant agreement nos. 101056939 (RESCUE) and 101183367 (NewPathWays)). In addition, this work has been partially funded by the European Union's Horizon Europe projects PRISMA (grant no. 101081604, J.P.D.) and OptimESM (grant no. 101081193, P.S.).

Author contributions

P.v.J and I.W. designed the study under the supervision of A.P. P.v.J., J.P.D., A.P., H.L.-C., P.S., F.H. and I.W. contributed to developing the MAgPIE model. J.A.J. developed and P.v.J. extended the SEALS model. P.v.J., T.M., P.B. and P.P. created the post-processing tools. P.v.J. produced and analysed the model outputs and prepared all figures and tables with feedback from I.W. and A.P. The paper was written by P.v.J. with contributions from all authors.

Funding

Open access funding provided by Potsdam-Institut für Klimafolgenforschung (PIK) e.V.

Competing interests

The authors declare no competing interests.

Additional information

Extended data is available for this paper at https://doi.org/10.1038/s41893-025-01595-9.

Supplementary information The online version contains supplementary material available at https://doi.org/10.1038/s41893-025-01595-9.

Correspondence and requests for materials should be addressed to Patrick von Jeetze.

Peer review information *Nature Sustainability* thanks Thomas Hertel, Koen Kuipers and Ana Carolina Fiorini for their contribution to the peer review of this work.

https://doi.org/10.1038/s41893-025-01595-9

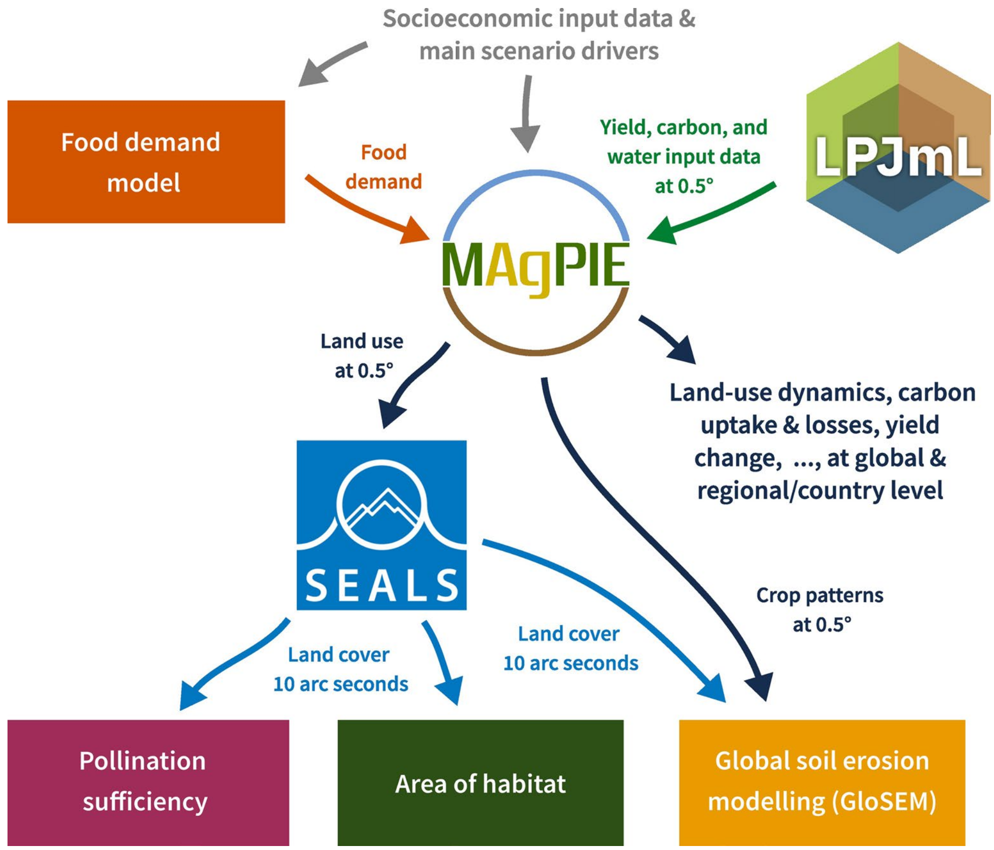

Extended Data Fig. 1 | The MAgPIE-SEALS modelling framework. MAgPIE uses a broad range of socioeconomic and spatially-explicit biophysical information to simulate global land system dynamics in the 21st century. Using empirically calibrated adjacency relationships, physical suitability and conversion eligibility information, SEALS allocates projected land cover changes to a spatial resolution that is suitable for assessing changes in biodiversity and the supply of important NCP.

https://doi.org/10.1038/s41893-025-01595-9

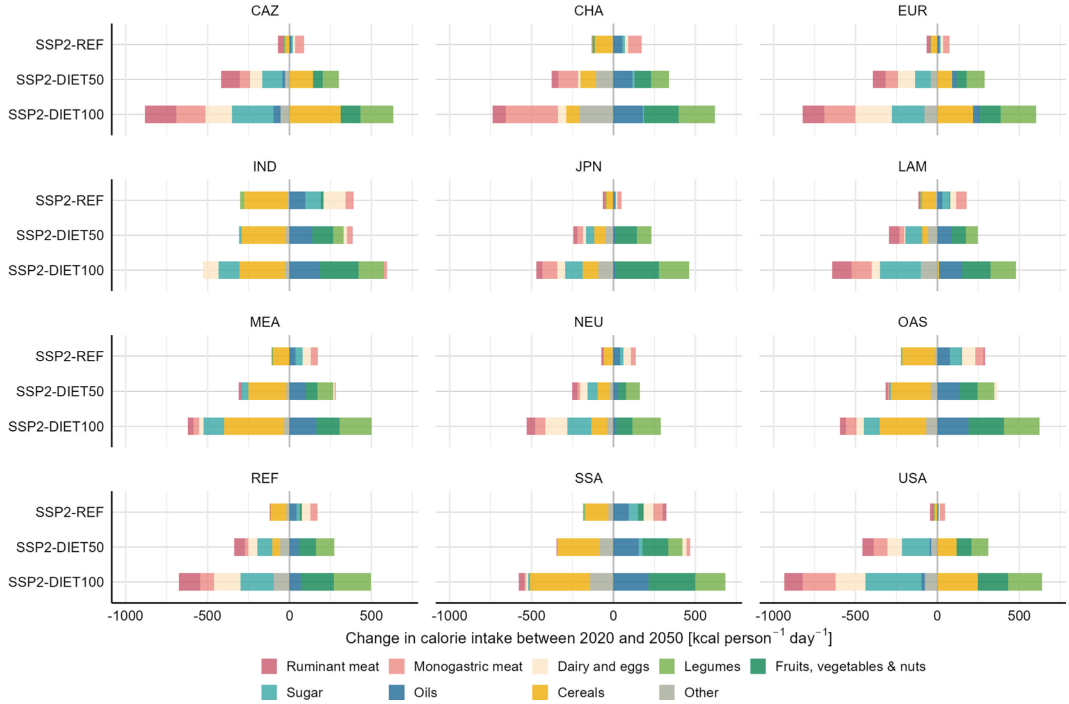

Extended Data Fig. 2 | Regional changes in calorie intake between 2020 and 2050 of different food groups and different convergence levels towards the healthy reference diet. CAZ: Canada, Australia and New Zealand; CHA: China; EUR: European Union; IND: India; JPN: Japan; LAM: Latin America; MEA: Middle East and Northern Africa; NEU: non-EU member states; OAS: other Asia; REF: reforming economies of the former Soviet Union; SSA: Sub-Saharan Africa; USA: United States.

https://doi.org/10.1038/s41893-025-01595-9

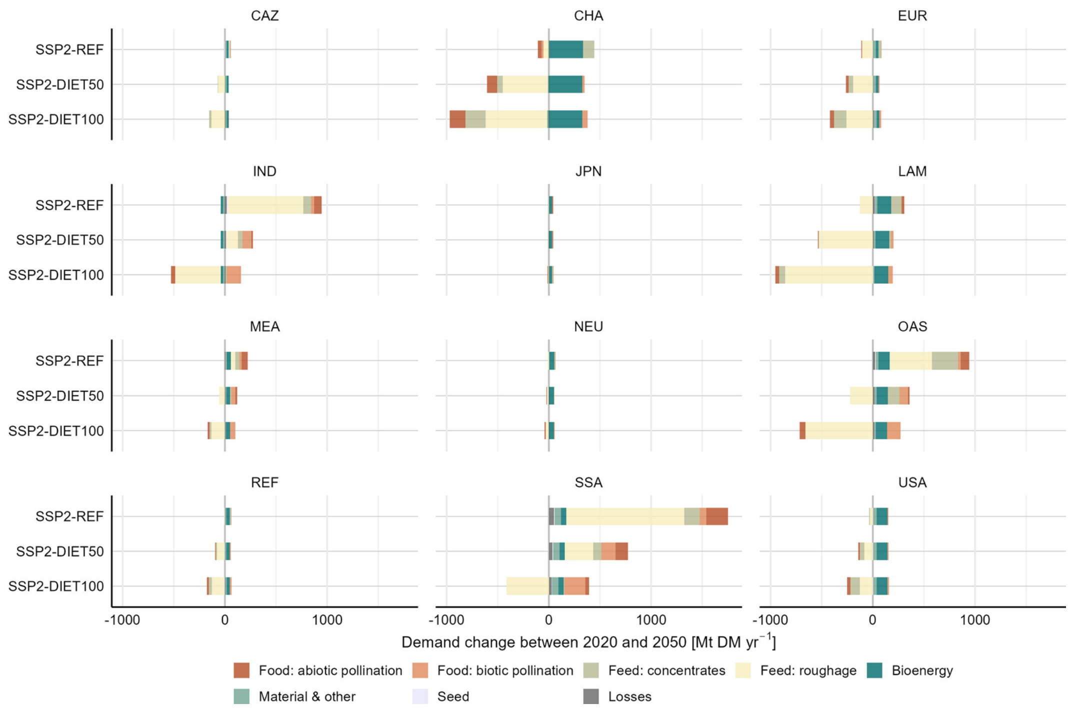

Extended Data Fig. 3 | Regional changes in agricultural demand between 2020 and 2050 for different convergence levels towards the healthy reference diet, separated into different commodity groups. CAZ: Canada, Australia and New Zealand; CHA: China; EUR: European Union; IND: India; JPN: Japan; LAM: Latin America; MEA: Middle East and Northern Africa; NEU: non-EU member states; OAS: other Asia; REF: reforming economies of the former Soviet Union; SSA: Sub-Saharan Africa; USA: United States.

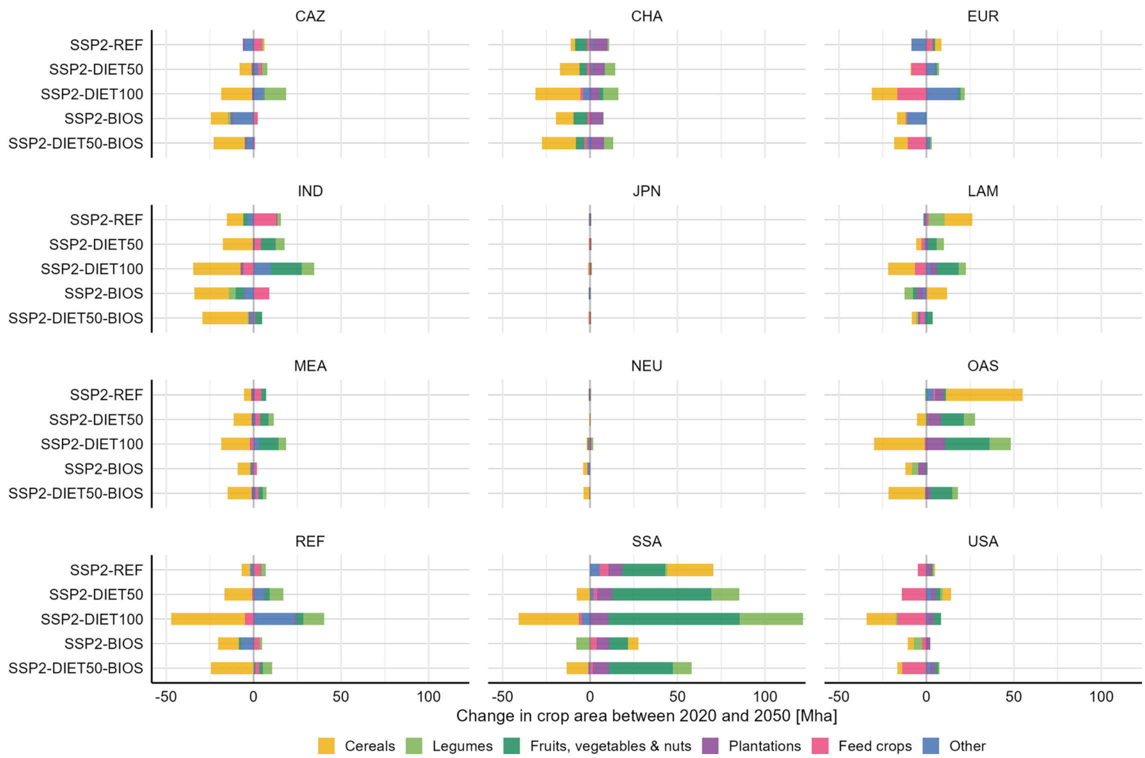

Extended Data Fig. 4 | Projected changes in regional crop area of different crop types between 2020 and 2050 across modelled land-system interventions. CAZ: Canada, Australia and New Zealand; CHA: China; EUR: European Union; IND: India; JPN: Japan; LAM: Latin America; MEA: Middle East and Northern Africa; NEU: non-EU member states; OAS: other Asia; REF: reforming economies of the former Soviet Union; SSA: Sub-Saharan Africa; USA: United States.

Extended Data Fig. 5 | Total sum of area of habitat losses between 2020 and 2050 caused by the reduction of aggregated land-use/land-cover (LULC) types across all assessed species. The sum of of global (**a**) regional (**b**) area of habitat losses is much higher than overall projected global and regional land-use changes, because one unit of expansion of each LULC type can cause AOH losses for several species. CAZ: Canada, Australia and New Zealand; CHA: China; EUR: European Union; IND: India; JPN: Japan; LAM: Latin America; MEA: Middle East and Northern Africa; NEU: non-EU member states; OAS: other Asia; REF: reforming economies of the former Soviet Union; SSA: Sub-Saharan Africa; USA: United States.

https://doi.org/10.1038/s41893-025-01595-9

Extended Data Fig. 6 | Regional number of species with more than 20% estimated area of habitat (AOH) loss by 2050 across modelled scenarios.

https://doi.org/10.1038/s41893-025-01595-9

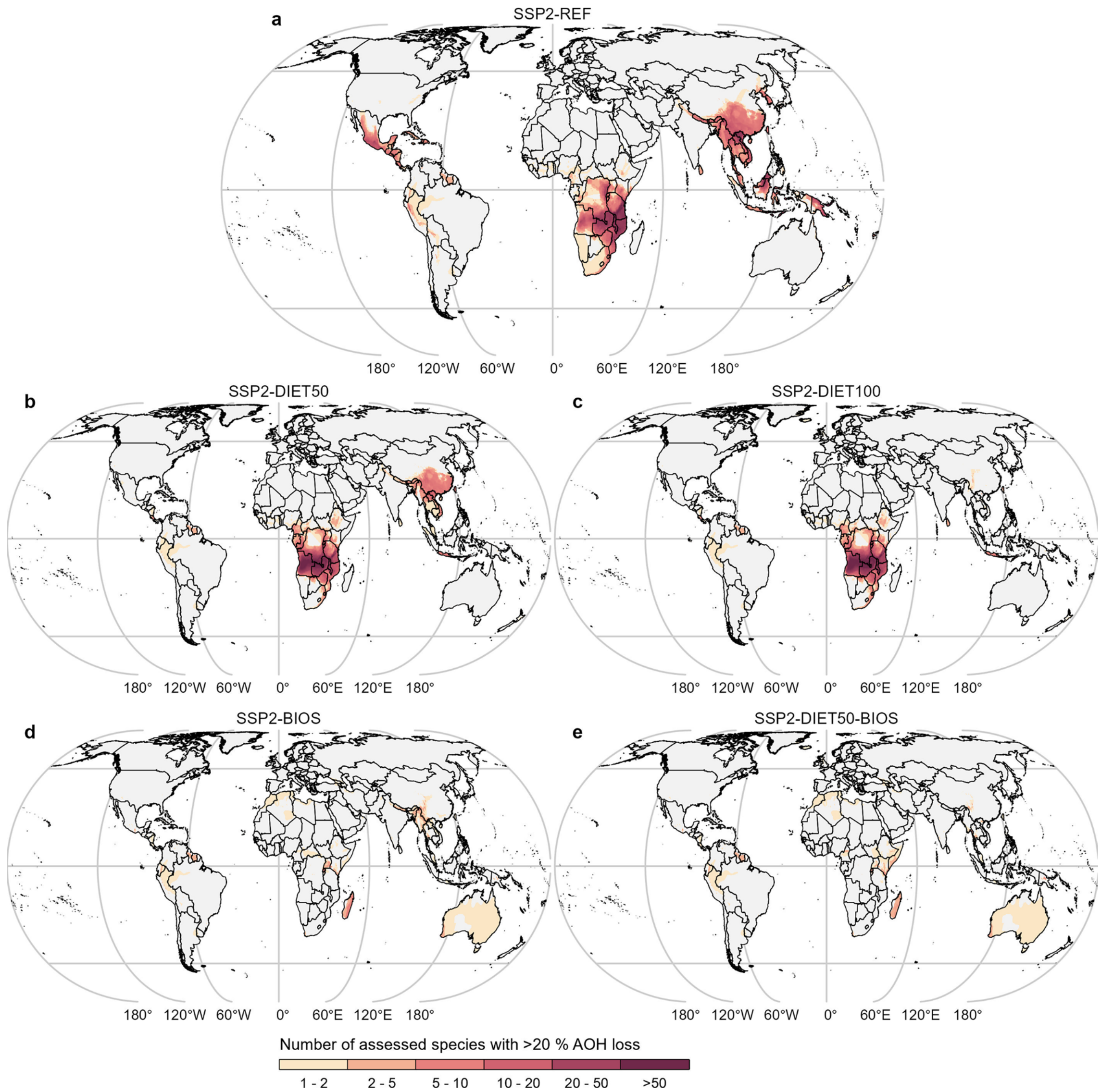

Extended Data Fig. 7 | Number of all assessed species with more than 20% habitat loss in 2050. The map shows the number of overlapping range polygons of all assessed vertebrate species affected by >20% habitat loss across all modelled scenarios (**a**-**e**). Country polygons were adapted from ref. 100. Basemaps adapted from World Bank Official Boundaries under a Creative Commons license CC BY 4.0.

https://doi.org/10.1038/s41893-025-01595-9

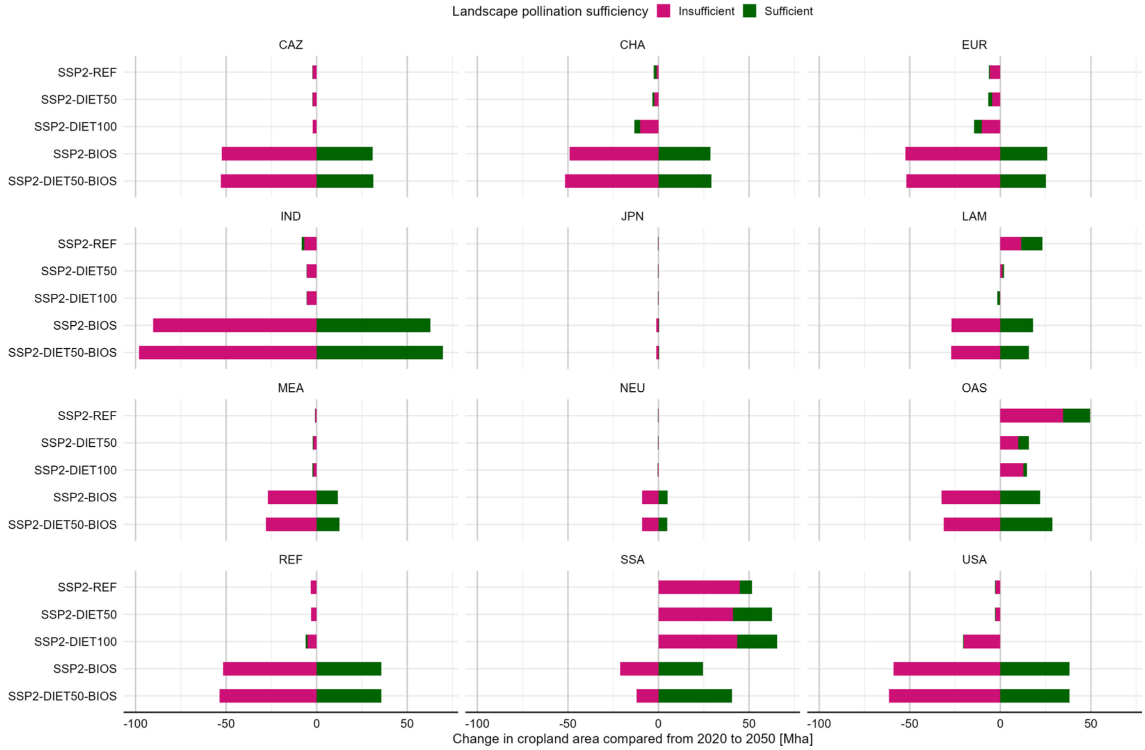

Extended Data Fig. 8 | Projected regional changes in landscape pollination sufficiency. CAZ: Canada, Australia and New Zealand; CHA: China; EUR: European Union; IND: India; JPN: Japan; LAM: Latin America; MEA: Middle East and Northern Africa; NEU: non-EU member states; OAS: other Asia; REF: reforming economies of the former Soviet Union; SSA: Sub-Saharan Africa; USA: United States.

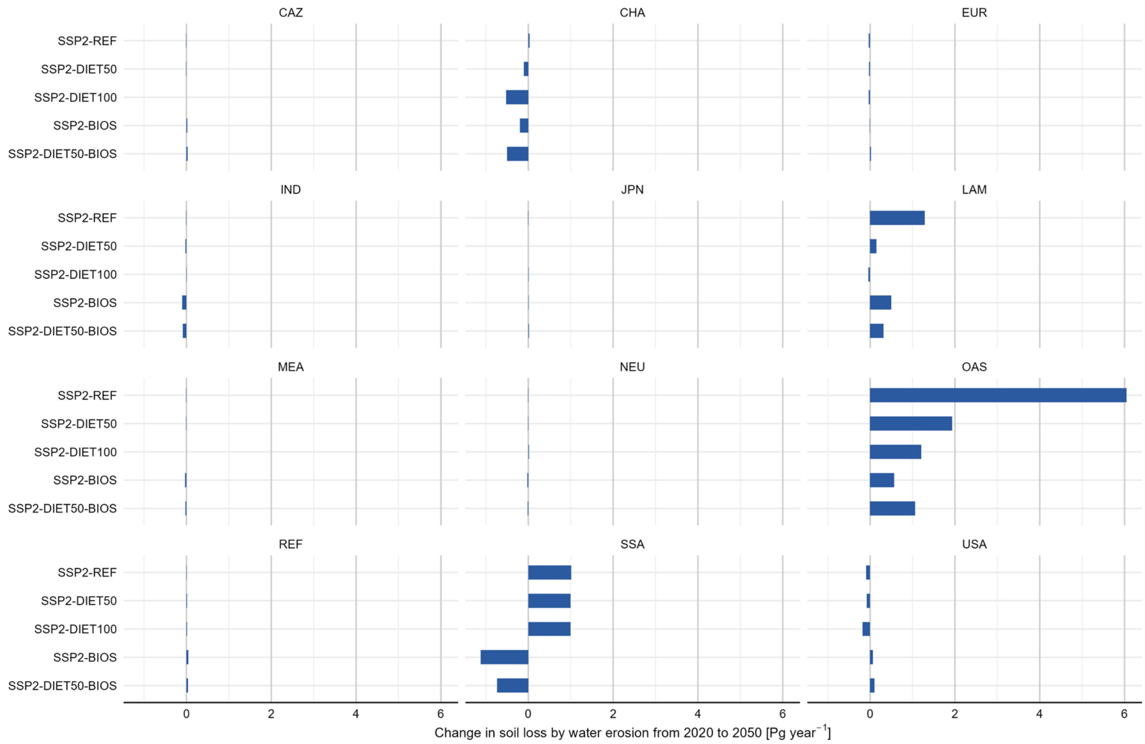

Extended Data Fig. 9 | Projected regional changes in soil loss by water erosion. CAZ: Canada, Australia and New Zealand; CHA: China; EUR: European Union; IND: India; JPN: Japan; LAM: Latin America; MEA: Middle East and Northern Africa; NEU: non-EU member states; OAS: other Asia; REF: reforming economies of the former Soviet Union; SSA: Sub-Saharan Africa; USA: United States.

https://doi.org/10.1038/s41893-025-01595-9

Extended Data Table 1 | Overview of main outcome indicators assessed in this study and their associated primary conservation value

Indicator and unit	Definition	Primary conservation value perspective	Reference
MAgPIE-SEALS			
Area of habitat (AOH) change (ha)	The area of habitat (AOH) refers to the habitat available to a species within its geographic range. AOH changes are derived for 6,374 amphibian, 9,124 bird, 5,351 mammal and 6,877 reptile species and are based on a fine-scale allocation of land-cover projections and corresponding changes in the suitable habitat. Range shifts due to climatic changes could not be considered here.	Nature for Nature	Brooks et al.[37], Lumbierres et al.[36,55]
Configurational landscape heterogeneity & pollination sufficiency (unitless)	Cropland pixels (300m x 300m) are ranked by values between 0 and 1. 1 indicates >30% semi-natural habitat within 2 km around cropland. Values between 0 to 1 indicate a proportion from 0 to 30%. The presence of semi-natural habitat has shown to be positively associated with a range of important NCP such as pollination supply[78,79] and an important driver of biodiversity[41].	Nature for Society	von Jeetze et al.[28], Chaplin-Kramer et al.[77]
Soil loss by water erosion (Pg year^{-1})	Soil loss by water erosion is estimated based on the Global Soil Erosion Modelling (GloSEM) platform. GloSEM is a large-scale Geographical Information System (GIS) version of the empirical, detachment-limited Revised Universal Soil Loss Equation (RUSLE) model. Soil loss by water erosion is a major driver of degradation of the supply of critical soil-related material and regulating NCP[43].	Nature for Society	von Jeetze et al.[28], Borrelli et al.[44]
MAgPIE			
CO_2 emissions from land-use change (Gt CO_2 year^{-1})	CO_2 emissions from land-use change include carbon losses to the atmosphere in terms of CO_2 from the conversion of pasture, forest and non-forest ecosystems, as well as carbon uptake due to vegetation growth and regrowth on abandoned or conserved land.	Nature for Society	Humpenöder et al.[18]
GHG emissions from AFOLU (Gt CO_2-eq year^{-1})	Agriculture, Forestry and Other Land Use (AFOLU) GHG emissions include CO_2 emissions from land-use change, N_2O emissions from agricultural soils and animal waste management, and CH_4 emissions from enteric fermentation, animal waste management and rice production. The CO_2 equivalents of N_2O and CH_4 emissions were calculated using IPCC AR6 GWP100 factors of 273 and 27 respectively.		Humpenöder et al.[45]
Average annual yield changes (% year^{-1})	The temporal development of agricultural yields is modelled endogenously based on cropland relocation and through the cost-effectiveness of investments into irrigation and research & development (R&D) investments into yield-increasing technological change relative to other cost components (e.g. land conversion or transport costs).		Dietrich et al.[75]
Expenditure on agricultural products (USD person^{-1} year^{-1})	Per capita expenditures in USD05 MER for agricultural commodities for food use, excluding the value-added in the supply chain. Food expenditure is derived from the country-level per-capita food use multiplied with the shadow price (Lagrange multiplier) of providing one additional unit of food in a world region.		Stevanović et al.[76]
Agricultural imports (Mt DM year^{-1})	A region imports agricultural commodities, if demand is not met by domestic production.		Schmitz et al.[68]

nature portfolio

Corresponding author(s): Patrick v. Jeetze

Last updated by author(s): Apr 17, 2025

Reporting Summary

Nature Portfolio wishes to improve the reproducibility of the work that we publish. This form provides structure for consistency and transparency in reporting. For further information on Nature Portfolio policies, see our Editorial Policies and the Editorial Policy Checklist.

Statistics

For all statistical analyses, confirm that the following items are present in the figure legend, table legend, main text, or Methods section.

n/a	Confirmed	
☒	☐	The exact sample size (*n*) for each experimental group/condition, given as a discrete number and unit of measurement
☒	☐	A statement on whether measurements were taken from distinct samples or whether the same sample was measured repeatedly
☒	☐	The statistical test(s) used AND whether they are one- or two-sided *Only common tests should be described solely by name; describe more complex techniques in the Methods section.*
☐	☒	A description of all covariates tested
☐	☒	A description of any assumptions or corrections, such as tests of normality and adjustment for multiple comparisons
☒	☐	A full description of the statistical parameters including central tendency (e.g. means) or other basic estimates (e.g. regression coefficient) AND variation (e.g. standard deviation) or associated estimates of uncertainty (e.g. confidence intervals)
☒	☐	For null hypothesis testing, the test statistic (e.g. *F*, *t*, *r*) with confidence intervals, effect sizes, degrees of freedom and *P* value noted *Give P values as exact values whenever suitable.*
☒	☐	For Bayesian analysis, information on the choice of priors and Markov chain Monte Carlo settings
☒	☐	For hierarchical and complex designs, identification of the appropriate level for tests and full reporting of outcomes
☒	☐	Estimates of effect sizes (e.g. Cohen's *d*, Pearson's *r*), indicating how they were calculated

Our web collection on statistics for biologists contains articles on many of the points above.

Software and code

Policy information about availability of computer code

Data collection	We linked the global land system modelling framework MAgPIE v4.8.2 (Model of Agricultural Production and its Impact on the Environment; written in GAMS and R) with the SEALS (Spatial Economic Allocation Landscape Simulator; written in Python) model. Globally gridded yield, carbon, and water input data was derived from the dynamic global vegetation, crop and hydrology model LPJmL (Lund-Potsdam-Jena managed Land; written in C++ and R). Our soil erosion estimates are based on the Global Soil Erosion Modelling (GloSEM) platform (implemented in R for this study). All models are referenced and described in more detail in the main manuscript. The model code of the MAgPIE model is openly available under the GNU Affero General Public License, version 3 (AGPLv3) and accessible via GitHub (https://github.com/magpiemodel/magpie). The release version (MAgPIE 4.8.2.), on which this study is based, has been archived via Zenodo (https://doi.org/10.5281/zenodo.13833444). MAgPIE 4.8.2. is accompanied by a technical model documentation (https://rse.pik-potsdam.de/doc/magpie/4.8.2/), which has been compiled with the GAMS code documentation toolkit goxygen.
Data analysis	Data analysis during post-processing was done in R by using the libraries 'luscale' v3.0.1, 'magpie4' v2.13.0 (both part of the MAgPIE modelling framework and accessible via https://github.com/pik-piam), 'terra' v1.7-81, 'exactextractr' v0.10.0, 'foreach' v1.5.2, 'doParallel' v1.0.17 (references provided in the manuscript).

For manuscripts utilizing custom algorithms or software that are central to the research but not yet described in published literature, software must be made available to editors and reviewers. We strongly encourage code deposition in a community repository (e.g. GitHub). See the Nature Portfolio guidelines for submitting code & software for further information.

Data

Policy information about availability of data

All manuscripts must include a data availability statement. This statement should provide the following information, where applicable:

- Accession codes, unique identifiers, or web links for publicly available datasets
- A description of any restrictions on data availability
- For clinical datasets or third party data, please ensure that the statement adheres to our policy

All model outputs used in this paper have also been archived via Zenodo and can be accessed under https://doi.org/10.5281/zenodo.10599895. All input data used in this study, such as the input data for the GloSEM platform, is fully referenced in the paper.

Human research participants

Policy information about studies involving human research participants and Sex and Gender in Research.

Reporting on sex and gender	No human research participants were involved in this study.
Population characteristics	n/a
Recruitment	n/a
Ethics oversight	n/a

Note that full information on the approval of the study protocol must also be provided in the manuscript.

Field-specific reporting

Please select the one below that is the best fit for your research. If you are not sure, read the appropriate sections before making your selection.

☐ Life sciences ☐ Behavioural & social sciences ☒ Ecological, evolutionary & environmental sciences

For a reference copy of the document with all sections, see nature.com/documents/nr-reporting-summary-flat.pdf

Ecological, evolutionary & environmental sciences study design

All studies must disclose on these points even when the disclosure is negative.

Study description	This study applies a spatially-explicit and empirically calibrated quantitative modelling approach to assess how a partial or full convergence to healthier diets at the global scale would affect indicators across different conservation perspectives and compares the outcomes to a set of alternative conservation measures.
Research sample	Our scenario set uses the 'middle of the road' shared socio-economic pathway (SSP2) assuming full compliance with currently implemented land policies, such as legally protected areas, as a reference case (SSP2-REF) and compares it to alternative scenarios assuming 50% (SSP2-DIET50) and 100% (SSP2-DIET100) convergence towards a healthy diet based on recommended intakes for legumes, sugars, fruits, vegetables, nuts and livestock products. Recommended intakes are expressed as maximum and minimum targets for each food group. Actual average dietary intakes may therefore still show considerable heterogeneity at country level. Additional scenarios include a proactive conservation scenario (SSP2-BIOS), which assumes both an expansion of protected areas in line with the targets specified in the Kunming-Montreal Global Biodiversity Framework (GBF) and a set of conservation measures outside protected areas, such as maintaining at least 20% semi-natural vegetation in agricultural landscapes, and lastly a combination of partial dietary change and targeted conservation measures (SSP2-BIOS-DIET50).
Sampling strategy	No new data was collected for this study.
Data collection	All relevant input data used and processed in this modelling study is fully documented in the manuscript or in openly available online documentations, referenced in the text.
Timing and spatial scale	We mainly provide a global analysis, but also indicate regional- or country-level outcomes. We also map and present spatially-explicit outcomes at an intermediate and a fine-scale spatial resolution of 0.5 degree (55x55 km at the equator) and 10 arc seconds ('field-scale'; 300x300 m at the equator).
Data exclusions	No data was excluded.
Reproducibility	The model code (https://doi.org/10.5281/zenodo.13833444) and the model outputs (https://doi.org/10.5281/zenodo.10599895) are available online.

Randomization	Not applicable as no new data was collected.
Blinding	Not applicable as no new data was collected.

Did the study involve field work? ☐ Yes ☒ No

Reporting for specific materials, systems and methods

We require information from authors about some types of materials, experimental systems and methods used in many studies. Here, indicate whether each material, system or method listed is relevant to your study. If you are not sure if a list item applies to your research, read the appropriate section before selecting a response.

Materials & experimental systems

n/a	Involved in the study
☒	☐ Antibodies
☒	☐ Eukaryotic cell lines
☒	☐ Palaeontology and archaeology
☒	☐ Animals and other organisms
☒	☐ Clinical data
☒	☐ Dual use research of concern

Methods

n/a	Involved in the study
☒	☐ ChIP-seq
☒	☐ Flow cytometry
☒	☐ MRI-based neuroimaging